The next steps for TMD fracture functions at CLAS12

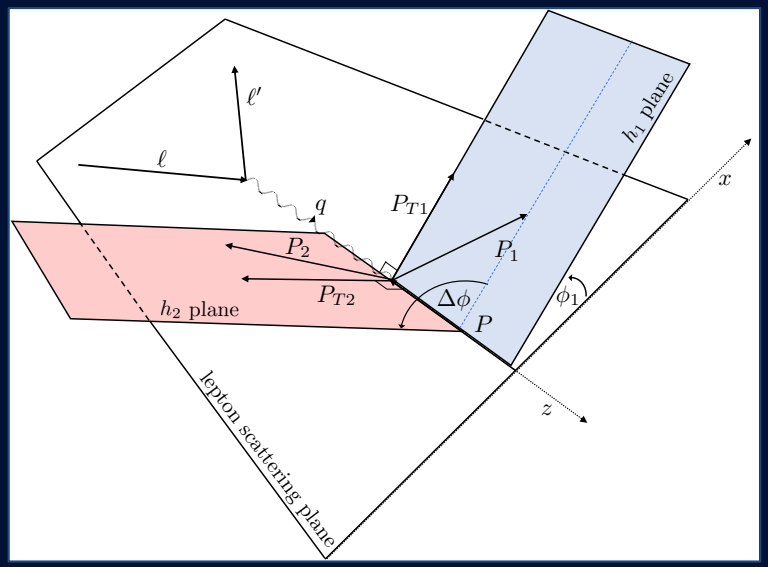

Timothy B. Hayward

March 22, 2023

Traditional SIDIS measurements

- Decades of study have led to detailed mappings of the momentum distribution of partons in the nucleon in terms of 1-D and 3-D (TMD) parton distribution functions (PDFs).
- Accessible in SIDIS measurements of cross sections and asymmetries, but rely on the assumption that measured hadrons are produced in the CFR.
- Cross section factorized[1] as a convolution of PDFs and Fragmentation Functions (FFs).

$$\frac{\mathrm{d}\sigma^{\mathrm{CFR}}}{\mathrm{d}x_B\,\mathrm{d}y\,\mathrm{d}z_h} = \sum_a e_a^2 \boxed{f_a(x_B)} \frac{\mathrm{d}\hat{\sigma}}{\mathrm{d}y} \boxed{D_a(z_h)}$$

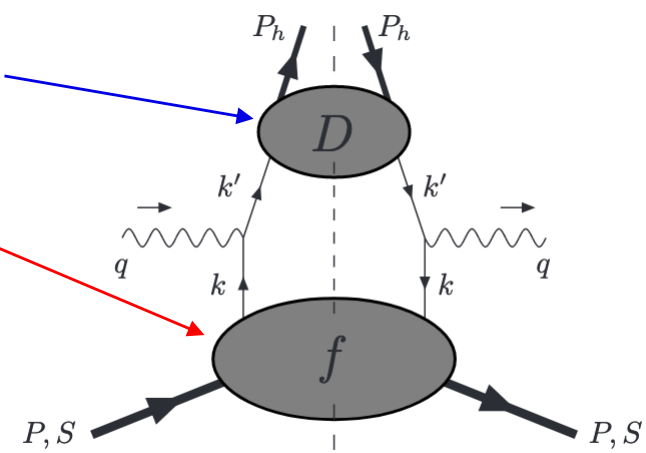

M. Anselmino et al., Phys. Lett. B. 706 (2011), 46-52, [hep-ph] 1109.1132

- PDFs
  - Probability (leading twist) of finding a particular parton in a certain configuration
  - Confined motion of quarks and gluons inside the nucleus
  - Orbital motion of quarks, correlations between quarks and gluons
- Fragmentation Functions
  - Nonperturbative dynamics of hadronization
  - Probability for a parton to form particular final state hadron
  - Insight into transverse momenta and polarization

1. A. Bacchetta et al., JHEP 02 (2007) 093 [hep-ph] 0611265,

The Neglected Hemisphere – Target Fragmentation

- Final state hadrons also form from the left-over target remnant (TFR) whose partonic structure is defined by "fracture functions"[1,2]: the probability for the target remnant to form a certain hadron given a particular ejected quark.
- In the TFR, factorization into x and z does not hold because it is not possible to separate quark emission from hadron production.

$$\frac{\mathrm{d}\sigma^{\mathrm{TFR}}}{\mathrm{d}x_B\,\mathrm{d}y\,\mathrm{d}z} = \sum_a e_a^2\,(1-x_B)\,\boxed{M_a(x_B,(1-x_B)z)}\,\frac{\mathrm{d}\hat{\sigma}}{\mathrm{d}y}$$

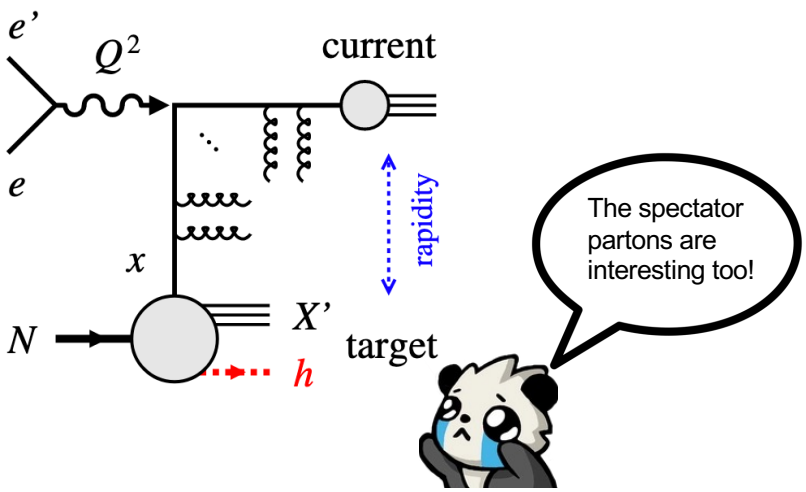

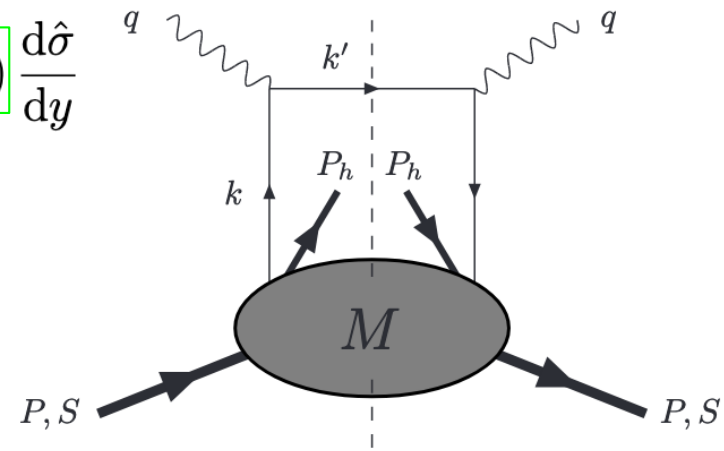

M. Anselmino et al., Phys. Lett. B. 706 (2011), 46-52, [hep-ph] 1109.1132

1. L. Trentadue and G. Veneziano, Phys. Lett. B323 (1994) 201,
2. M. Anselmino et al., Phys. Lett. B. 699 (2011), 108-118, [hep-ph] 1102.4214
3. TFR/CFR Fig. from EIC Yellow Report, (2021) [physics.ins-det] 2103.05419

Categorizing Fracture Functions

- At leading twist fracture functions exist that can be organized into tables of quark and nucleon polarizations just like the more familiar PDFs.
- Access to *both* k_T and p_T effects gives 2 x 8 = 16 FrFs.

Quark polarization

Nucleon polarization	U	L	T
U	f_1		$h_1^\perp$
L		g_{1L}	$h_{1L}^\perp$
T	$f_{1T}^\perp$	g_{1T}	$h_1, h_{1T}^\perp$

CFR ⟷ TFR

Quark polarization

Nucleon polarization	U	L	T
U	$\hat{u}_1$	$\hat{l}_1^{\perp h}$	$\hat{t}_1^h, \hat{t}_1^\perp$
L	$\hat{u}_{1L}^{\perp h}$	$\hat{l}_{1L}$	$\hat{t}_{1L}^h, \hat{t}_{1L}^\perp$
T	$\hat{u}_{1T}^h, \hat{u}_{1T}^\perp$	$\hat{l}_{1T}^h, \hat{l}_{1T}^\perp$	$\hat{t}_{1T}, \hat{t}_{1T}^{hh}$ $\hat{t}_{1T}^{\perp\perp}, \hat{t}_{1T}^{\perp h}$

M. Anselmino et al., Phys. Lett. B. 706 (2011), 46-52, [hep-ph] 1109.1132

Analogs to PDFs

- A direct relationship exists to the eight leading twist PDFs after the fracture functions are integrated over the fractional longitudinal nucleon momentum.

$$z(1-x) = E_h/E = \zeta$$

$$\sum_h \int d\zeta M_a(x_B)(x_B, k_\perp^2, \zeta) = (1-x_B) f_a(x_B, k_\perp^2)$$

M. Anselmino et al., Phys. Lett. B. 699 (2011), 108, [hep-ph] 1102.4214

Quark polarization

Nucleon polarization	U	L	T
U	f_1		$h_1^\perp$
L		g_{1L}	$h_{1L}^\perp$
T	$f_{1T}^\perp$	g_{1T}	$h_1, h_{1T}^\perp$

unpolarized analog

helicity analog

etc. etc.

Quark polarization

Nucleon polarization	U	L	T
U	$\hat{u}_1$	$\hat{l}_1^{\perp h}$	$\hat{t}_1^h, \hat{t}_1^\perp$
L	$\hat{u}_{1L}^{\perp h}$	$\hat{l}_{1L}$	$\hat{t}_{1L}^h, \hat{t}_{1L}^\perp$
T	$\hat{u}_{1T}^h, \hat{u}_{1T}^\perp$	$\hat{l}_{1T}^h, \hat{l}_{1T}^\perp$	$\hat{t}_{1T}, \hat{t}_{1T}^{hh}$ $\hat{t}_{1T}^{\perp\perp}, \hat{t}_{1T}^{\perp h}$

M. Anselmino et al., Phys. Lett. B. 706 (2011), 46-52, [hep-ph] 1109.1132

Why fracture functions?

- Sometimes possible to kinematically separate CFR and TFR (some jets, high energy DY, etc) … but not always clear (fixed target experiments).
- Without an understanding of the signals we expect from target fragmentation we may misinterpret results that we expect are from the current.
- Studying the TFR tests our complete understanding of the SIDIS production mechanism while also providing access to information not available in the CFR.
- Access to more familiar TMD/PDFs through momentum sum rules, but with different systematics.

Single hadron limitations

- FrFs describing transversely polarized quarks are chiral odd and inaccessible in TFR single hadron production where there is no access to a chiral odd FF.
- Functions with double superscripts containing h and ⊥ have give the unique possibility of measuring longitudinal polarized quarks in unpolarized nucleons (and vice versa) but disappear after integration over either momentum.

Quark polarization

Nucleon polarization	U	L	T
U	f_1		$h_1^\perp$
L		g_{1L}	$h_{1L}^\perp$
T	$f_{1T}^\perp$	g_{1T}	$h_1, h_{1T}^\perp$

CFR ⟷ TFR

Quark polarization

Nucleon polarization	U	L	T
U	$\hat{u}_1$	$\hat{l}_1^{\perp h}$	$\hat{t}_1^h, \hat{t}_1^\perp$
L	$\hat{u}_{1L}^{\perp h}$	$\hat{l}_{1L}$	$\hat{t}_{1L}^h, \hat{t}_{1L}^\perp$
T	$\hat{u}_{1T}^h, \hat{u}_{1T}^\perp$	$\hat{l}_{1T}^h, \hat{l}_{1T}^\perp$	$\hat{t}_{1T}, \hat{t}_{1T}^{hh}$ $\hat{t}_{1T}^{\perp\perp}, \hat{t}_{1T}^{\perp h}$

M. Anselmino et al., Phys. Lett. B. 706 (2011), 46-52, [hep-ph] 1109.1132

First b2b publication

- When two hadrons are produced "back-to-back"[1,2] with one in the CFR and one in the TFR the structure function contains a convolution of a fracture function and a fragmentation function.

1. L. Trentadue and G. Veneziano, Phys. Lett. B323 (1994) 201,
2. M. Anselmino et al., Phys. Lett. B. 699 (2011), 108-118, [hep-ph] 1102.4214

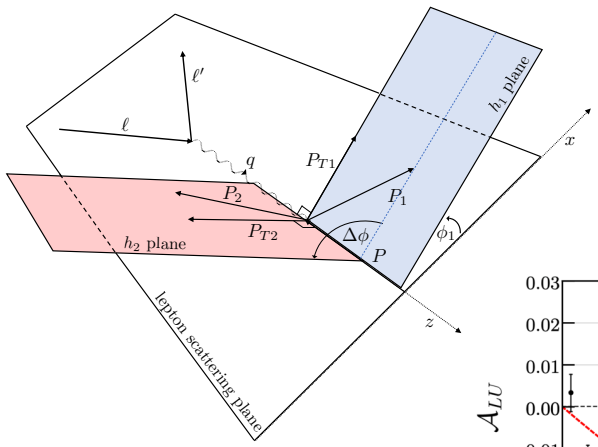

$\hat{l}_1^{\perp h}$

$$A_{LU} = -k(\epsilon)\frac{P_{T1}P_{T2}}{m_1 m_2}\frac{\mathcal{C}\left[w_5 \hat{l}_1^{\perp h}(x,\zeta_2,P_{T2})D_1(z_1,P_{T1})\right]}{\mathcal{C}\left[\hat{u}_1(x,\zeta_2,P_{T2})D_1(z_1,P_{T1})\right]}\sin(\Delta\phi)$$

Unique access to longitudinally polarized quarks in unpolarized nucleon… no corresponding PDF!

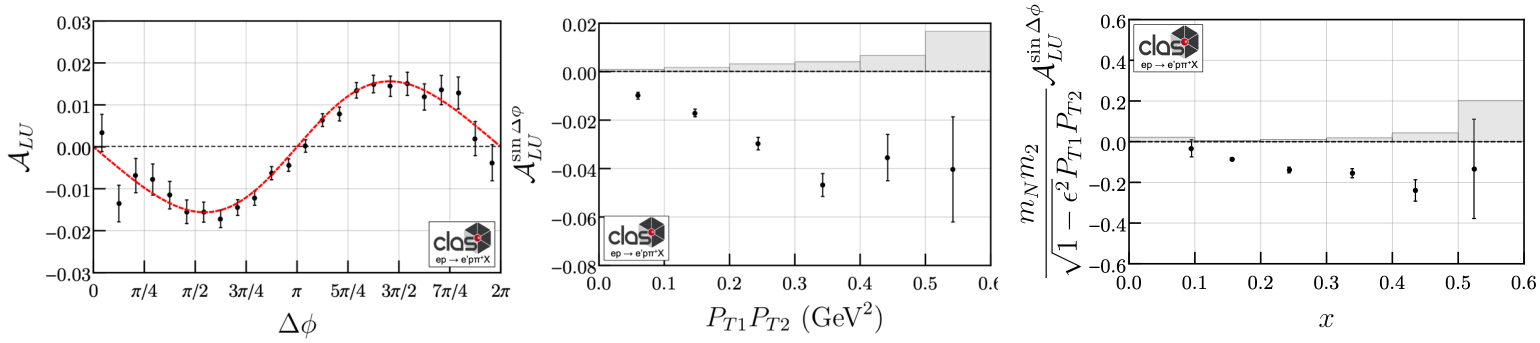

H. Avakian, T. Hayward, et al., Phys.Rev.Lett. 130 (2023) 2, 022501

Analysis Plan

CONTENTS

Analysis note nearly complete.

Leading twist fracture function describing the hadronization of the target remnant after ejection of a longitudinally polarized quark from an unpolarized nucleus.

$$A_{LU} = -k(\epsilon)\frac{P_{T1}P_{T2}}{m_1 m_2}\frac{\mathcal{C}\left[w_5 \hat{l}_1^{\perp h}(x,\zeta_2,P_{T2})D_1(z_1,P_{T1})\right]}{\mathcal{C}\left[\hat{u}_1(x,\zeta_2,P_{T2})D_1(z_1,P_{T1})\right]}\sin(\Delta\phi)$$

Convolution of fracture function (TFR hadron) and fragmentation function (CFR hadron).

Also new for this analysis:

1. Proton energy loss
2. Statistically relevant multidimensional binning
3. Flavor decomposition of target and produced pions
4. Q^2 evolution
5. etc.

	RGA In	RGA Out	RGB In	RGB Out
ep -> e'pπ^+X	PRL, PRD	PRD	PRD	PRD
ep -> e'pπ^-X	PRD	PRD	PRD	PRD

clas

UCONN

Sampling fraction drift due to PMT gain drift

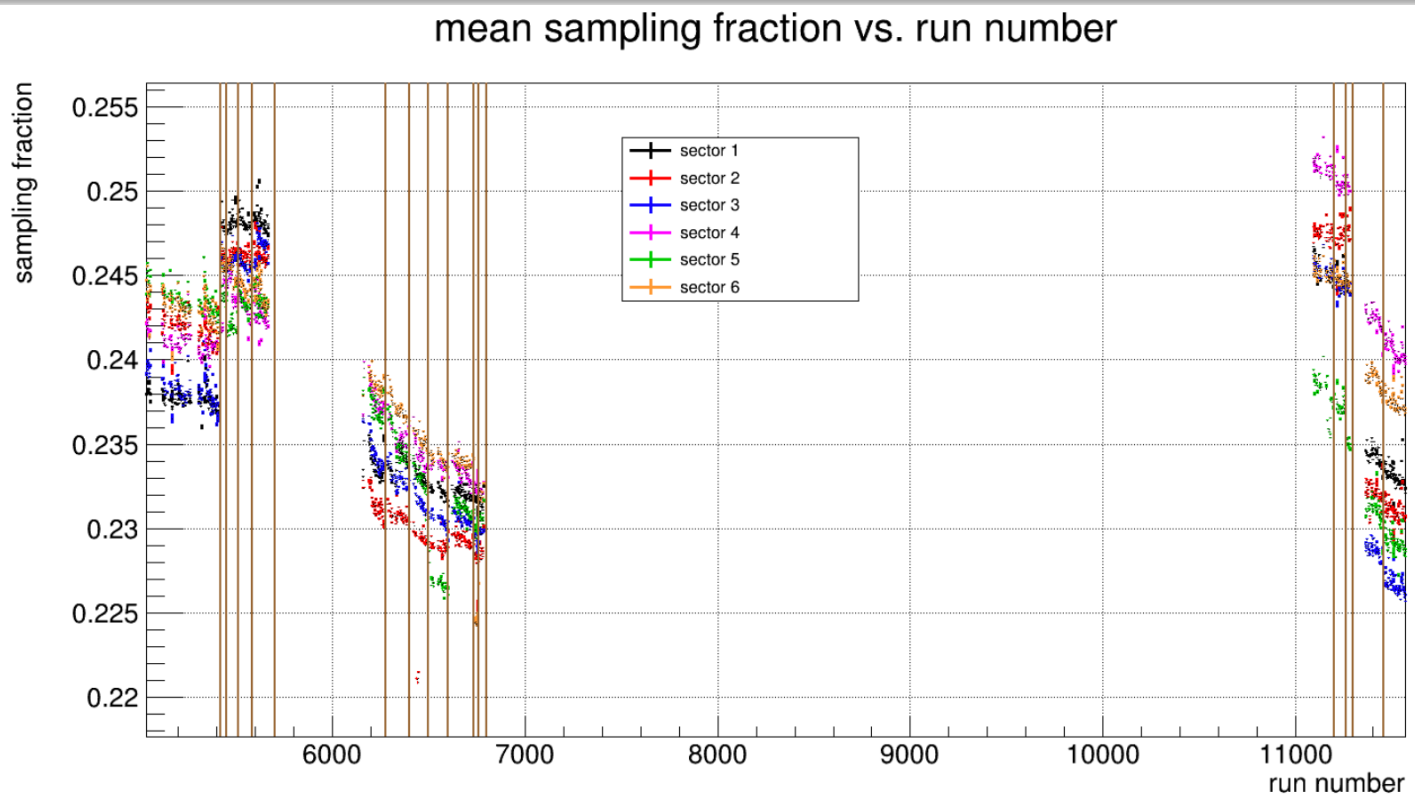

- Vertical lines = epoch boundaries, where an epoch has a “somewhat” constant S.F.
- Could implement epoch-dependent S.F. cuts

Sampling Fraction Cut

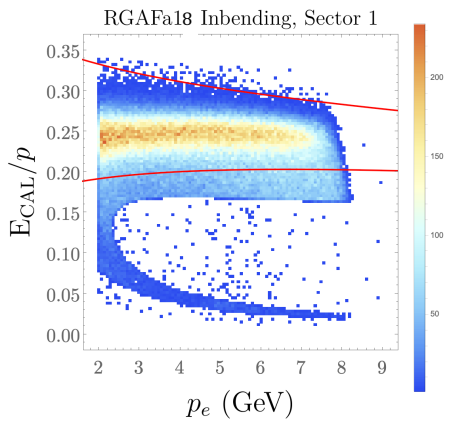

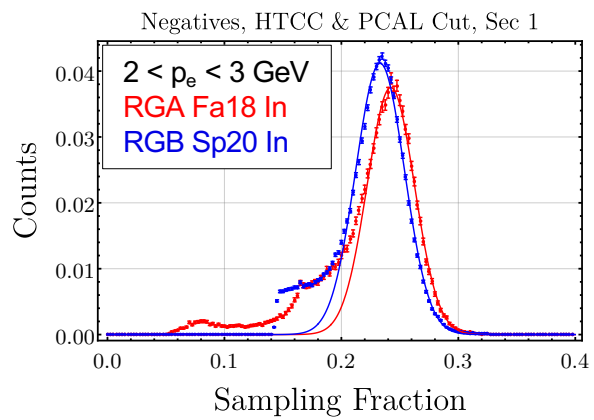

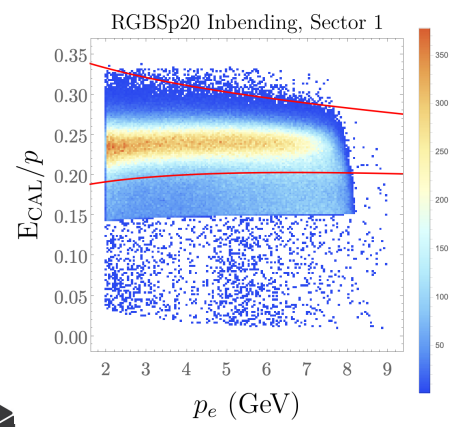

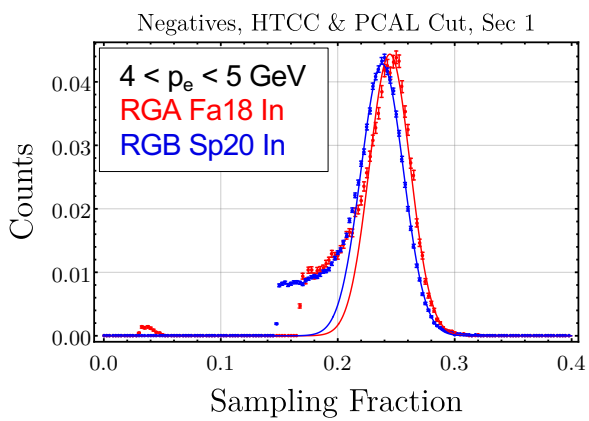

- Slightly different sampling fraction cuts for different run periods. Effect almost negligible on final selection.

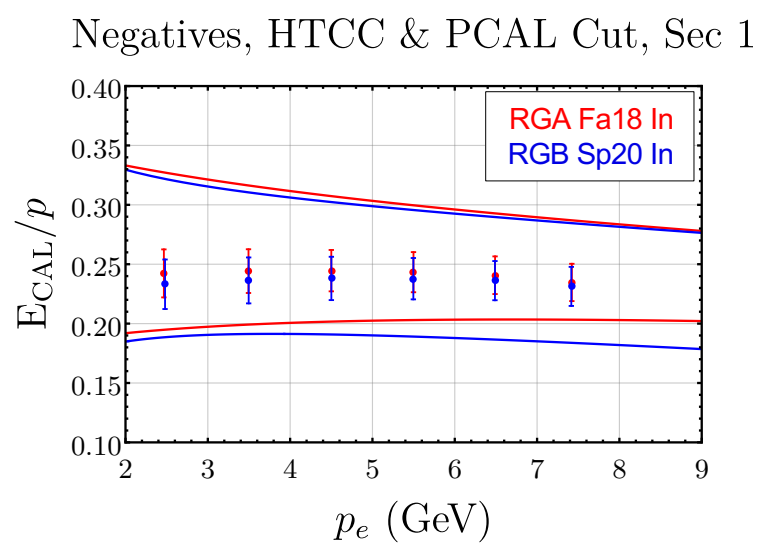

Sampling Fraction Sector Dependence

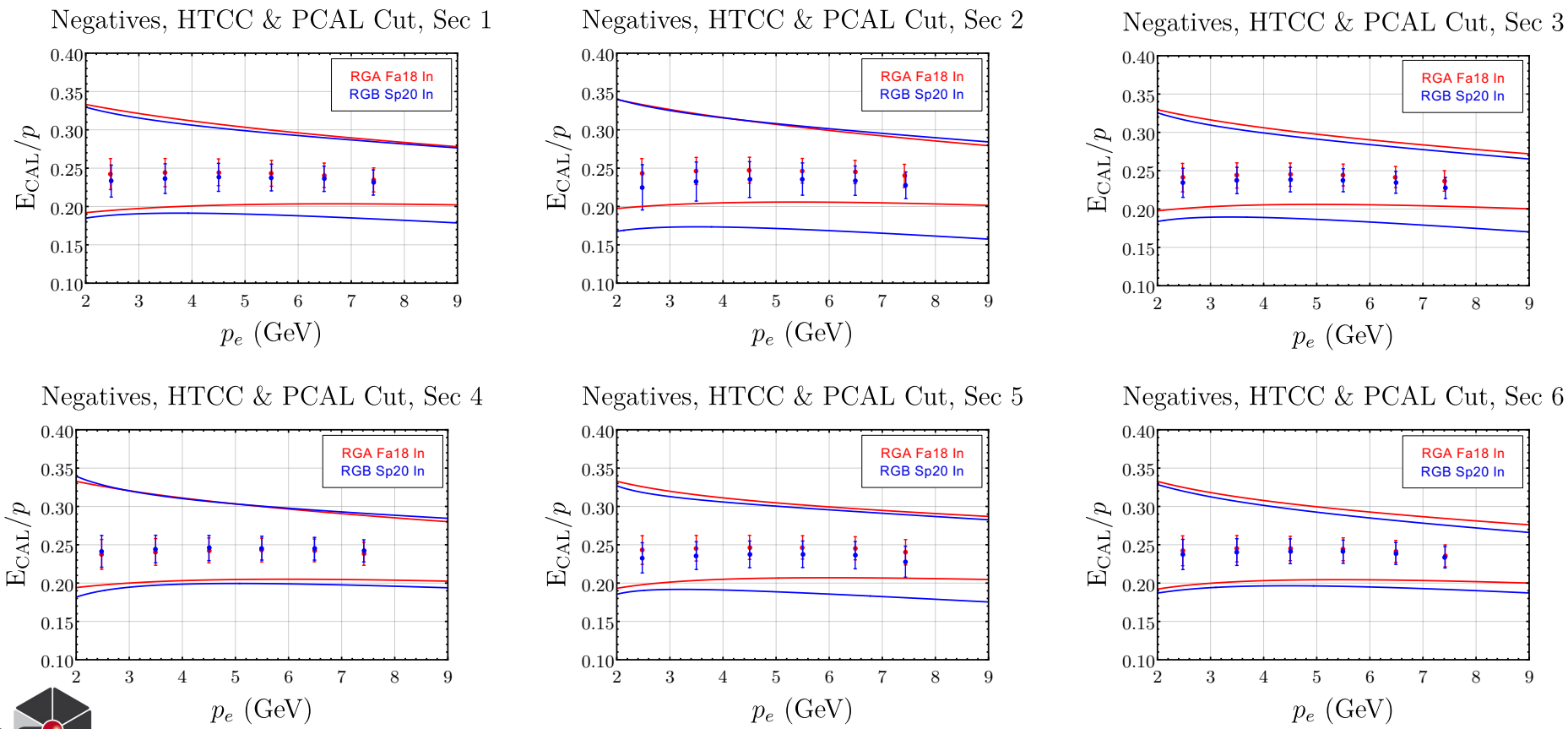

Hadron ID

FTOF calibrations are remarkably consistent across all 6 run periods → use RGA momentum dependent chi2pid cut for pions and |chi2pid| < 3 for protons.

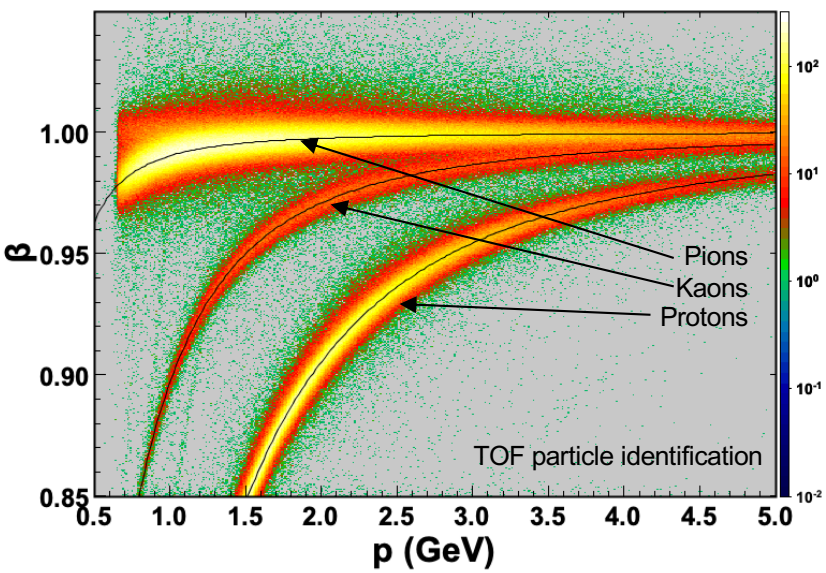

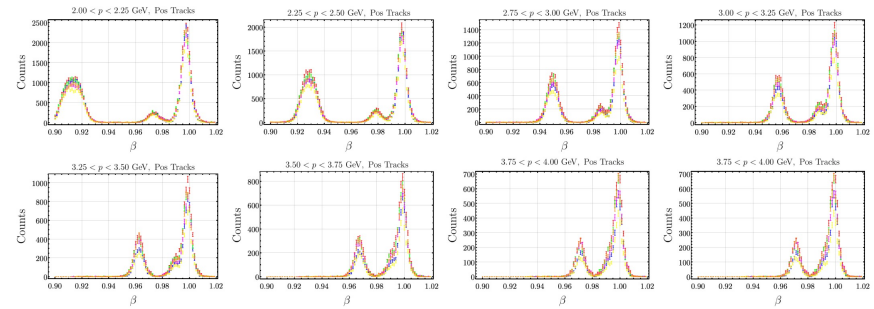

FIG. 18: One dimensional slices of the β distributions of positive tracks in various momentum bins for RGAFa18In (red), RGAFa18Out (blue), RGASp19In (green), RGBSp19In (magenta), RGBFa18Out (yellow) and RGBSp20In (orange).

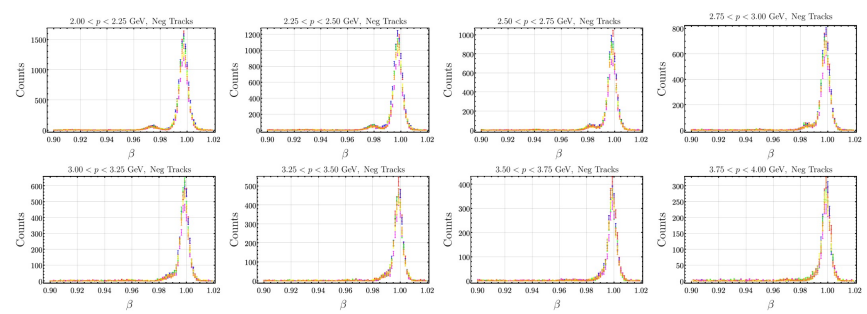

FIG. 19: One dimensional slices of the β distributions of negative tracks in various momentum bins for RGAFa18In (red), RGAFa18Out (blue), RGASp19In (green), RGBSp19In (magenta), RGBFa18Out (yellow) and RGBSp20In (orange).

Combining torus polarities

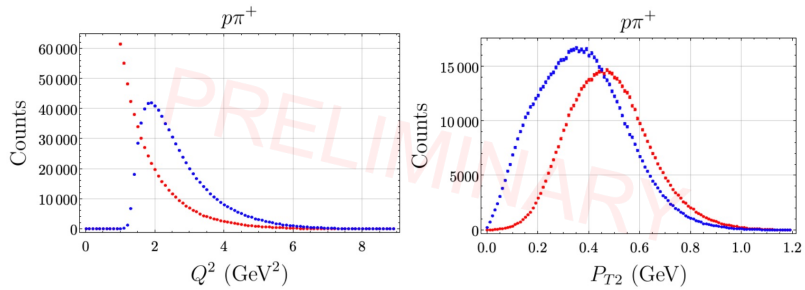

FIG. 7: The Q^2 (left) and P_{T2} (right) distributions for inbending (blue) and outbending (red) data.

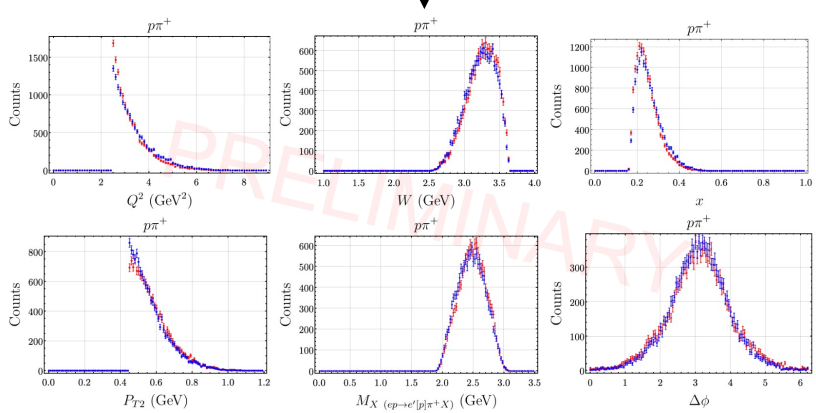

FIG. 8: Inbending (blue) and outbending (red) data for the Q^2, W, x, P_{T2}, M_X and $\Delta\phi$ distributions following cuts on the data of $Q^2 > 2.5$ GeV^2 and P_{T1} and $P_{T2} > 0.45$ GeV.

Inbending and outbending results are consistent in the overlapping kinematic regions.

Inbending
Outbending

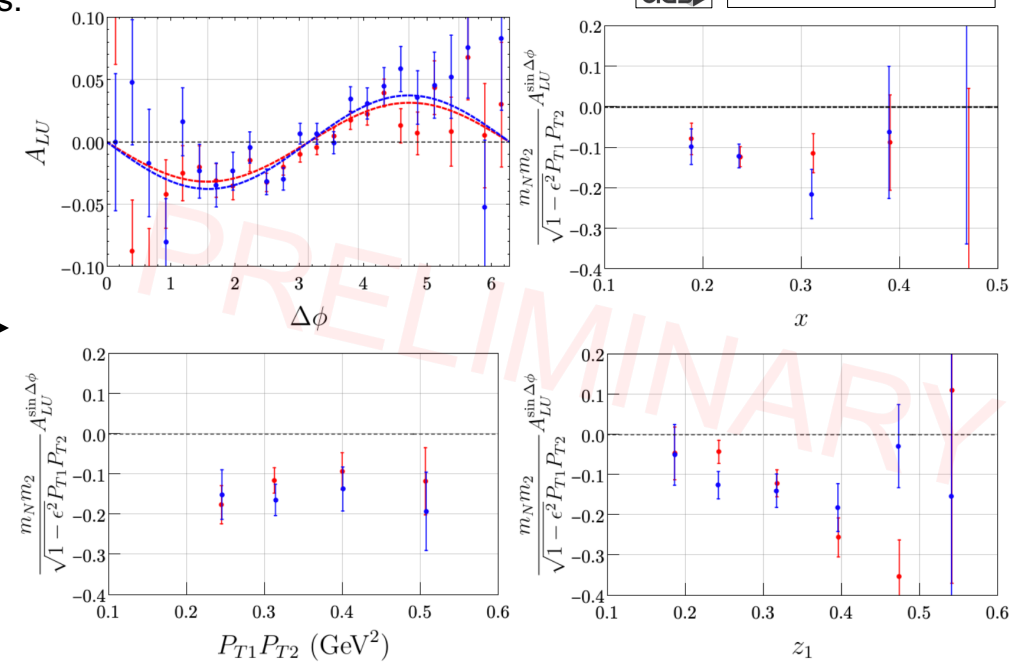

FIG. 9: Inbending (blue) and outbending (red) amplitude extractions for the integrated asymmetry, x, $P_{T1}P_{T2}$ and z_1 following cuts on the data of $Q^2 > 2.5$ GeV^2 and P_{T1} and $P_{T2} > 0.45$ GeV.

Baryonic Resonances

If both hadrons are from the same parent, then the event cannot be part of the back-to-back formalism.

1. $\Delta^{++} \rightarrow p\pi^+$
2. $\Delta^0 \rightarrow p\pi^-$
3. $N^{*0}(1520) \rightarrow p\pi^-$
4. $N^{*0}(1680) \rightarrow p\pi^-$

No N^*s in $p\pi^+$ channel because of charge conservation.

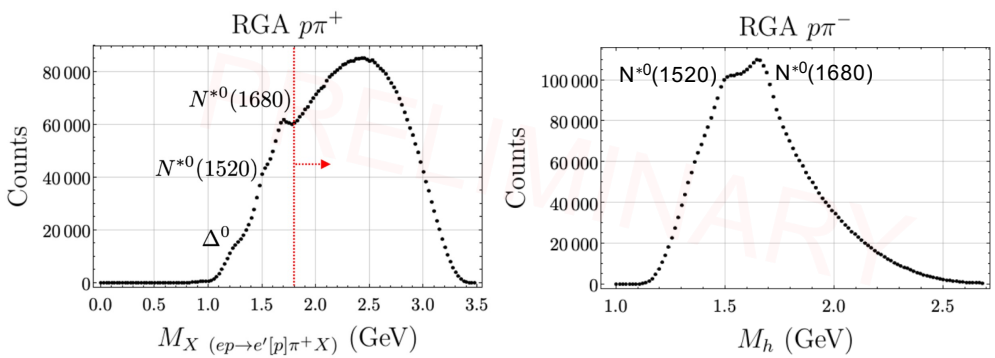

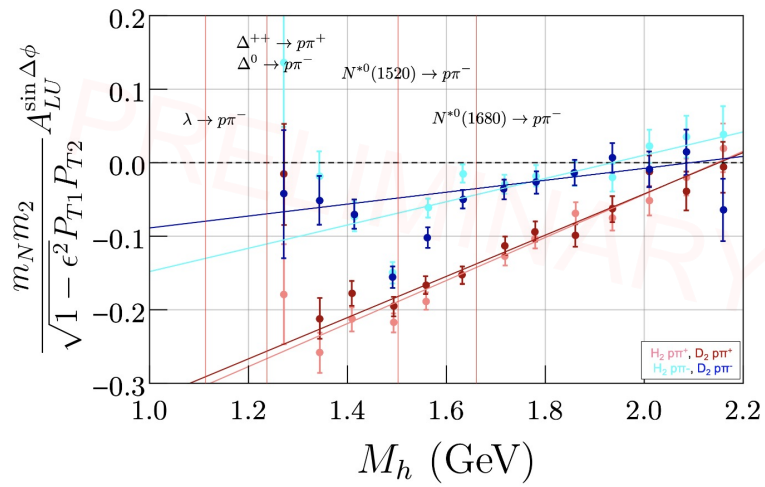

FIG. 56: The RGA $p\pi^+$ channel in pink, RGB $p\pi^+$ channel in red, RGA $p\pi^-$ channel in cyan and RGB $p\pi^-$ channel in blue. Each line with a matching color to its data set corresponds to a linear fit of the $M_h > 1.8$ GeV points (the area uncontaminated by same-parent decays). Vertical thin red lines are labeled where various baryon or nucleon resonances decay directly to decay products analyzed in this study.

At first glance, the N^{*0} in particular seem to have a large effect on the asymmetry…

Background or kinematic quirk?

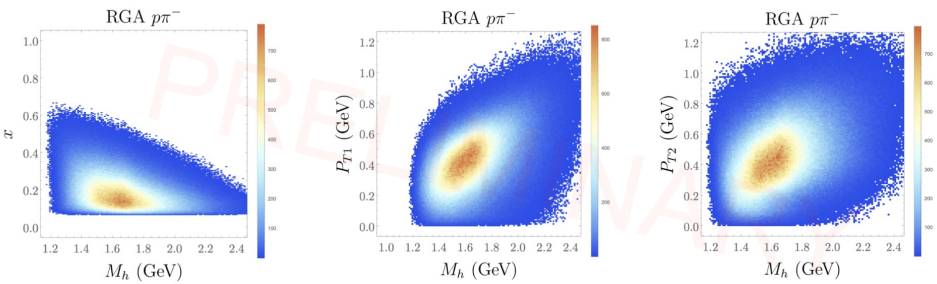

FIG. 30: 2D correlation plots between $M_{p\pi^-}$ and x (left), P_{T1} (center) and P_{T2} (right).

As M_h increases x decreases (asymmetries decrease) but P_T increases (asymmetries increase)…

RGA $p\pi^-$

M_h	x	P_{T1}	P_{T2}	$P_{T1}P_{T2}$
1.27152	0.274326	0.390832	0.265444	0.108485
1.34199	0.236334	0.376196	0.280935	0.104242
1.41489	0.218817	0.390206	0.305443	0.114542
1.48885	0.203354	0.415468	0.332263	0.131966
1.56279	0.190489	0.448527	0.365185	0.158305
1.63747	0.179379	0.480389	0.401353	0.188846
1.71061	0.171863	0.508493	0.433292	0.217986
1.78581	0.163357	0.533137	0.464615	0.247309
1.86095	0.158319	0.555573	0.494057	0.275283
1.93514	0.152569	0.578697	0.523222	0.307552
2.00998	0.148572	0.593513	0.554084	0.33465
2.08418	0.141026	0.613425	0.581181	0.363577
2.15947	0.136358	0.630251	0.615032	0.399424

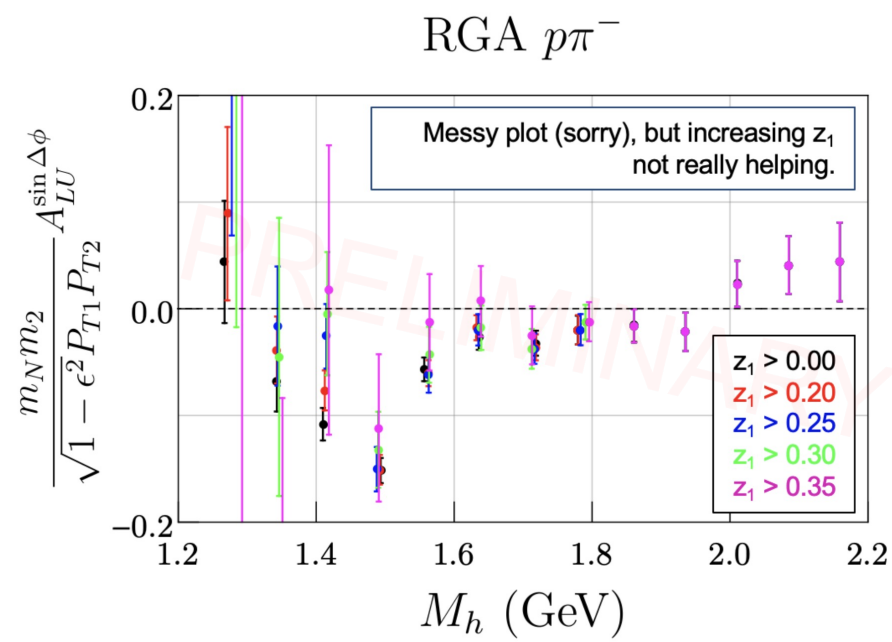

Increasing minimum required z_1 (which should decrease contributions from TFR pions) seems to have no effect.

Estimating as a systematic

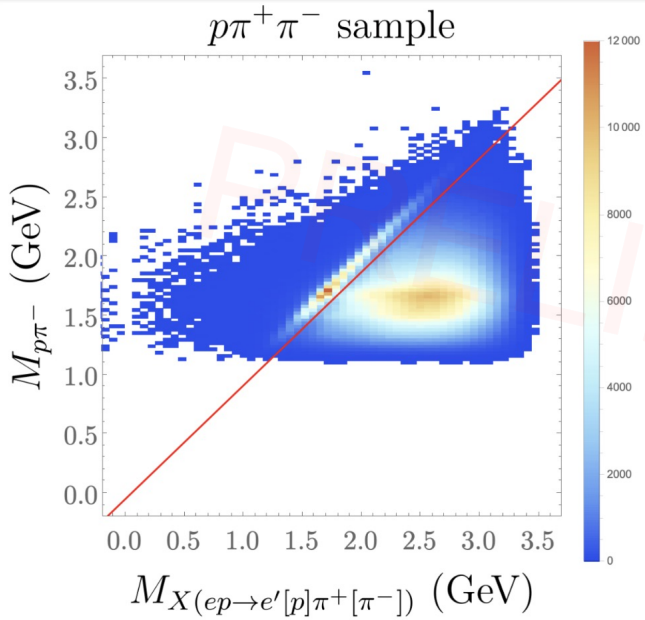

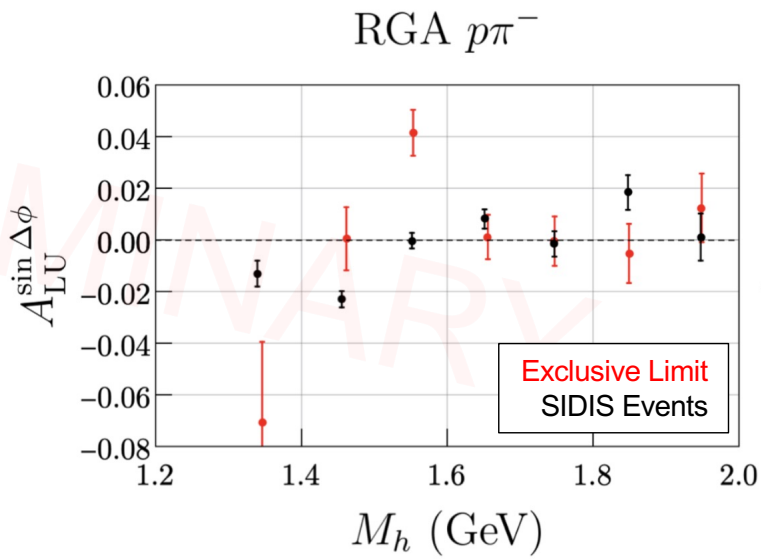

- Exclusive events possess larger amplitudes than SIDIS (i.e. exclusive limit).
- Exclusive events are easily identifiable in the "trihadron" ($ep\to e'p\pi^+\pi^-X$) sample.
- Exclusive asymmetries **have the opposite sign** as would be expected if the "dip" is truly due to N* events.
- Use exclusive limit to place upper bound on systematic, ~2-5% scale systematic depending on bin.

Target Flavor Comparison

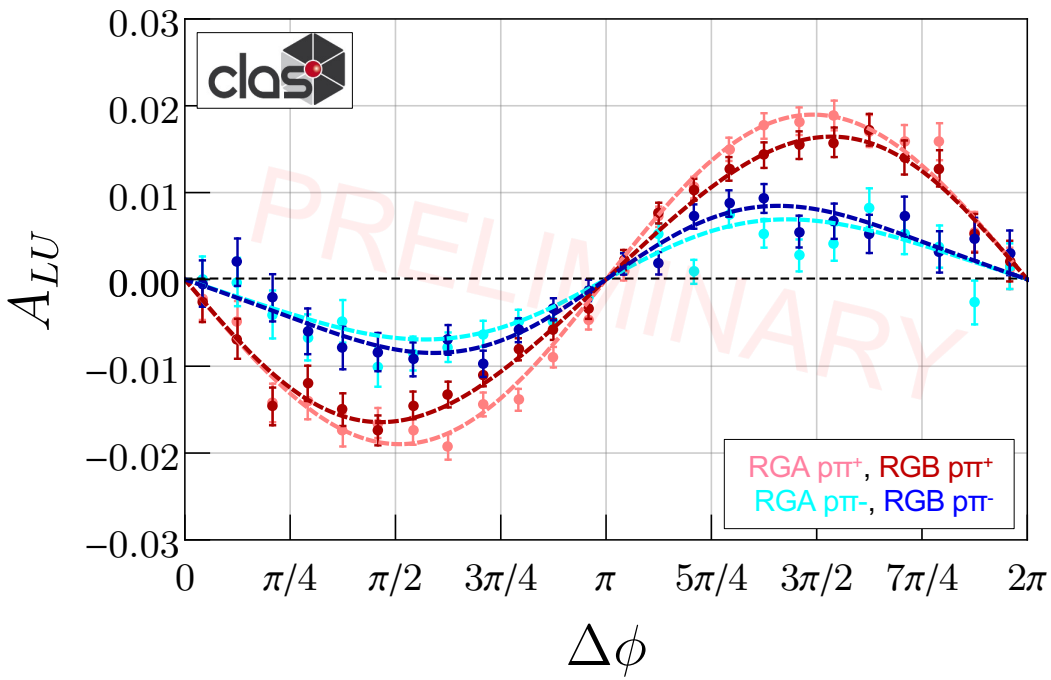

1. Asymmetries off the proton and deuteron are statistically consistent throughout all of parameter space (compare with e.g. ep(d)→e'$\pi^+\pi^-$X)
2. Asymmetry is a true valence quark effect!

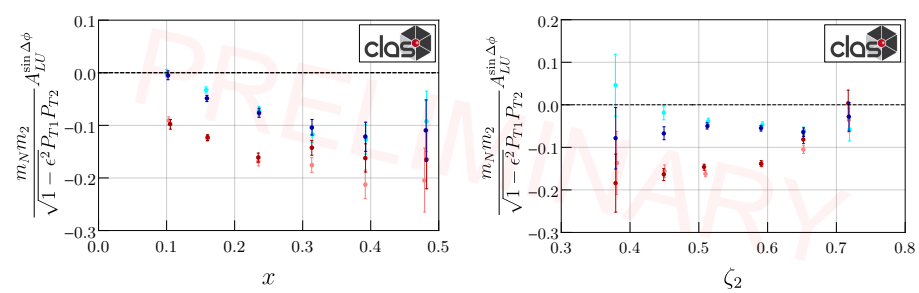

Pion Flavor Comparison

1. Significant flavor dependence on the pion is observed.
2. Similar trend to other SIDIS observables → π^+ and π^- asymmetries have same sign where vector mesons dominate and opposite signs where direct production dominates (e.g. high and low P_{T1} dependence).
3. Correlations between proton and vector mesons appear to be stronger than directly produced pions.

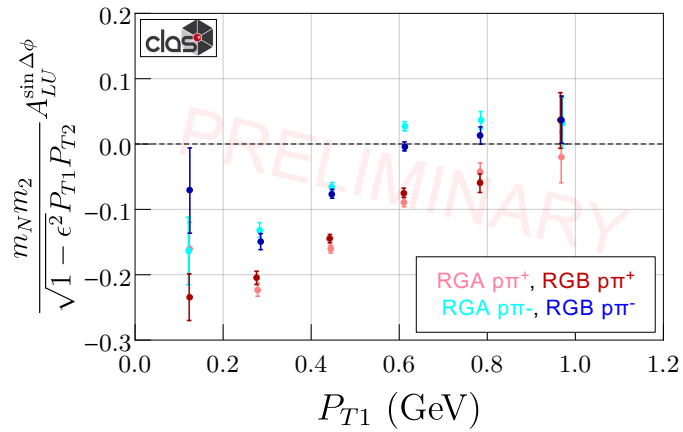

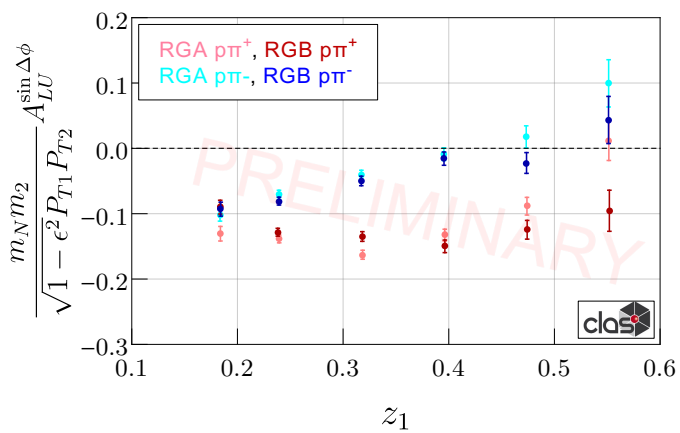

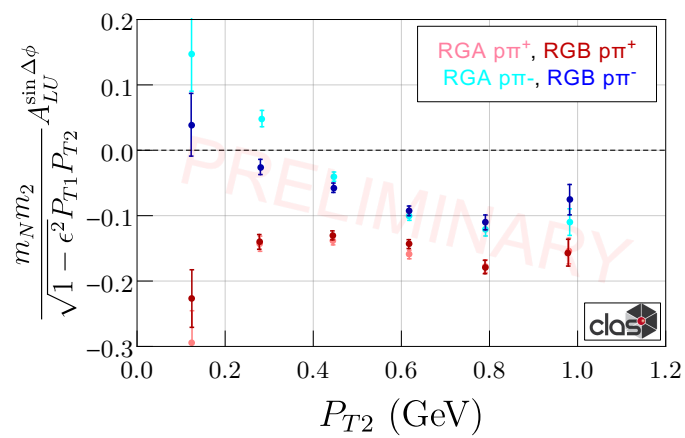

Verifying leading-twist behavior

1. sin(Δϕ) asymmetry is expected to be leading twist (no suppression in Q^2).
2. Multidimesional binning in Q^2 and x required.
3. Behavior consistent with flat dependence on Q^2.
4. JLab22 would allow for a significant extension of Q^2 coverage.

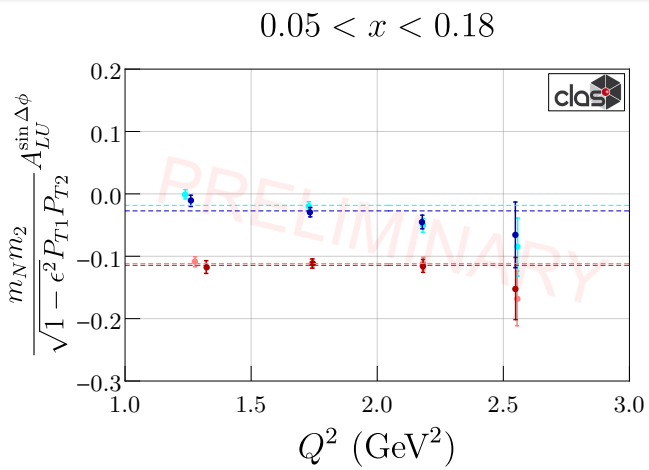

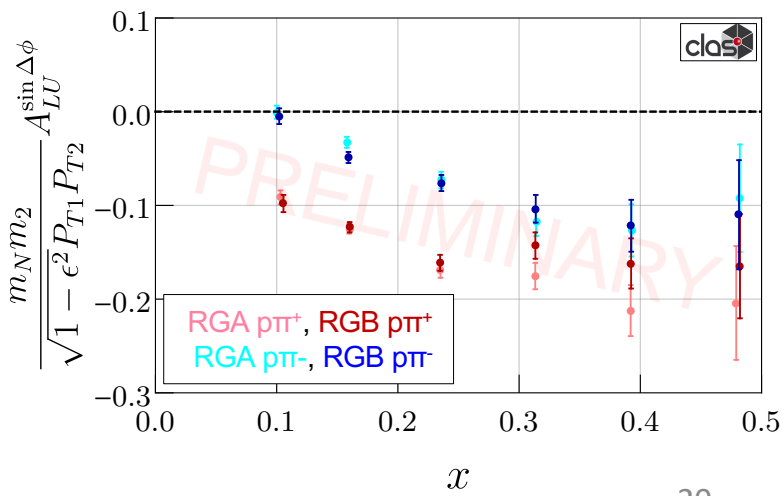

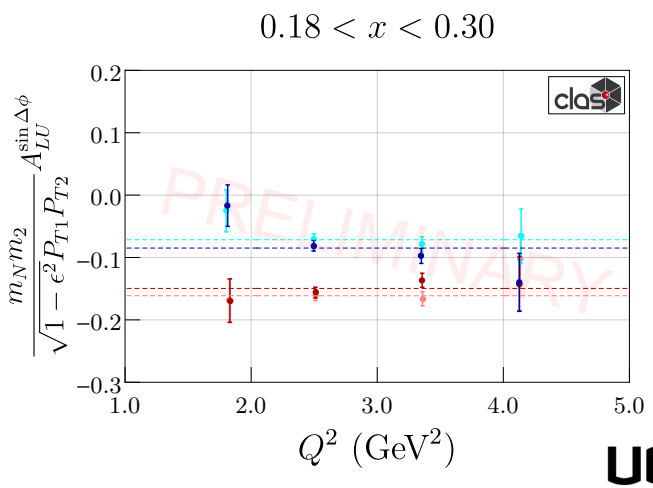

A_{LL} – The Best of Both Worlds

$$\frac{d\sigma}{dx dy d\zeta dP_T^2} = 2\pi\hat{\sigma}_U \sum_q e_q^2 \left[F_{UU,T} + \lambda S_L \sqrt{1-\varepsilon^2} F_{LL}\right]$$

M. Anselmino et al., Phys. Lett. B. 699 (2011), 108, [hep-ph] 1102.4214

At leading twist for the case of a longitudinally polarized target and a single hadron produced in the TFR, only two terms appear:

$$F_{UU,T} \propto \tilde{u}_1(x,\zeta,P_T^2) = \int d^2k_T \hat{u}_1$$

$$F_{LL} \propto \tilde{l}_{1L}(x,\zeta,P_T^2) = \int d^2k_T \hat{l}_{1L}$$

J.J. Ethier et al., *Phys. Rev. Lett.*, 119, (2017), [hep:ph 1705.05889]

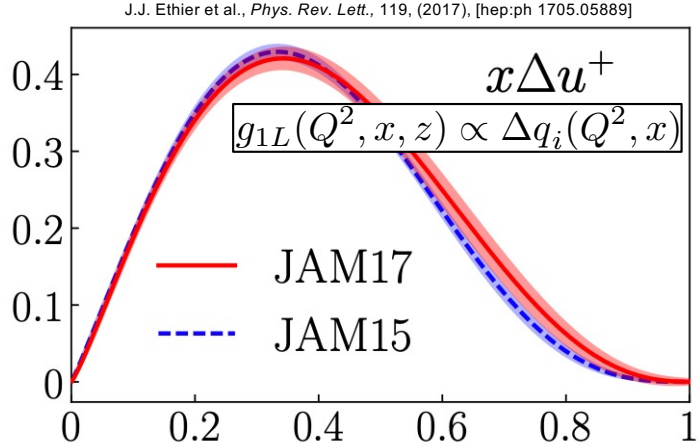

Double Spin Asymmetry: $A_{LL} = \lambda_\ell S_L \frac{\sqrt{1-\epsilon^2} F_{LL}}{F_{UU,T}}$

1. Single hadron → Highest statistics
2. Leading twist → Simple interpretation
3. Linked to g_1 → easiest test of FrF prediction

$$\sum_h \int \zeta d\zeta \int d^2P_T \hat{l}_{1L} = (1-x) g_{1L}(x,k_T^2)$$

Integrated epX asymmetries

- Six inbending FT-on configuration RGC runs were analyzed.
- RGA Fa18 PID used; M_x > 1.40 GeV (avoid exclusive events)
- $n^{\pm\pm}$ weighted by total accumulated charge.
- Dilution factor estimated from MC.
- Very preliminary, but behavior is as expected!

$$A_{LU} = \frac{1}{P_b}\frac{P_t^-(n^{++}-n^{-+})+P_t^+(n^{+-}-n^{--})}{P_t^-(n^{++}+n^{-+})+P_t^+(n^{+-}+n^{--})}$$

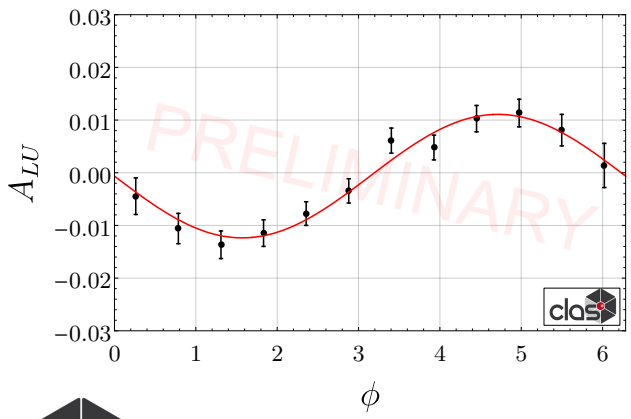

$$A_{UL}^{\text{lab}} = \frac{1}{D_f}\frac{(n^{++}+n^{-+})-(n^{+-}+n^{--})}{P_t^-(n^{++}+n^{-+})+P_t^+(n^{+-}+n^{--})}$$

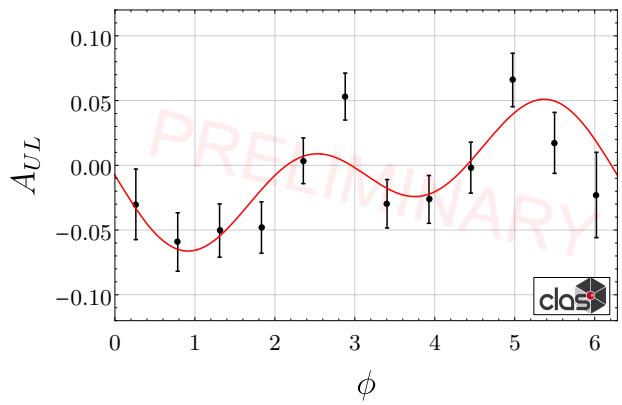

$$A_{LL}^{\text{lab}} = \frac{1}{P_b D_f}\frac{(n^{++}-n^{-+})+(n^{--}-n^{+-})}{P_t^-(n^{++}+n^{-+})+P_t^+(n^{+-}+n^{--})}$$

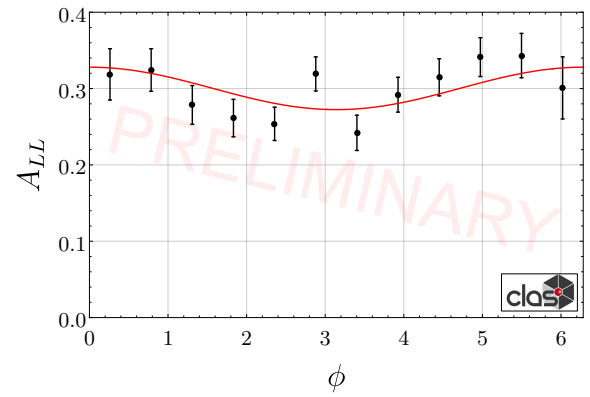

Transition from TFR to CFR

TFR

$$(\gamma_\perp \cdot \tilde{P}_{h\perp})_{ij} \hat{u}_{2L}^{\perp h}(x, \xi, P_{h\perp})$$

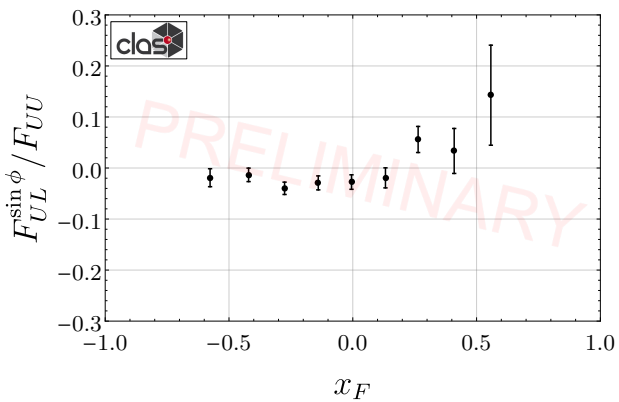

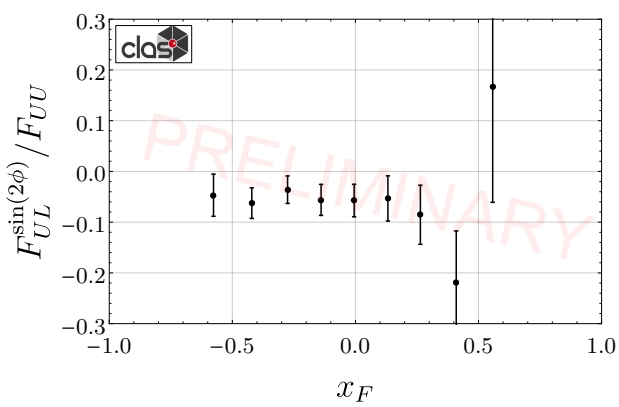

No Collins function so $F_{UL}^{\sin(2\phi)}$ and $F_{UU}^{\cos(2\phi)}$ are pure twist-4 terms in the TFR

CFR

$$F_{UL}^{\sin\phi_h} = \frac{2M}{Q}\mathcal{C}\left[-\frac{\hat{\boldsymbol{h}}\cdot\boldsymbol{k}_T}{M_h}\left(xh_L H_1^\perp + \frac{M_h}{M} g_{1L}\frac{\tilde{G}^\perp}{z}\right) + \frac{\hat{\boldsymbol{h}}\cdot\boldsymbol{p}_T}{M}\left(xf_L^\perp D_1 - \frac{M_h}{M} h_{1L}^\perp \frac{\tilde{H}}{z}\right)\right]$$

Sign flip indicative of odd-function transition from FrF to PDF/FF formalism (consistent with preliminary BSAs from RGA).

$$F_{UL}^{\sin 2\phi_h} = \mathcal{C}\left[-\frac{2\left(\hat{\boldsymbol{h}}\cdot\boldsymbol{k}_T\right)\left(\hat{\boldsymbol{h}}\cdot\boldsymbol{p}_T\right) - \boldsymbol{k}_T\cdot\boldsymbol{p}_T}{MM_h} h_{1L}^\perp H_1^\perp\right]$$

Kotzinian-Mulders asymmetry is twist 2 in the CFR. Rapid increase in magnitude indicative of transition from twist-4 TFR to twist-2 CFR?

Conclusions

- Studies of the TFR and correlations between the TFR and CFR are crucial for gaining an understanding of hadronization and for accurately evaluating systematics arising from oversimplified assumptions about independent fragmentation.
- Back-to-back RGA Inbending proton-π^+ beam-spin asymmetries recently published in PRL.
- Significant extension involving the outbending data, RGB and additional pion flavors nearly complete.
- Next steps:
  1. Finalize RGA e'pX beam-spin asymmetries.
  2. Transition to the longitudinally polarized target: A_{UL} and A_{LL} for inclusive e'pX and e'pπ^+X, both of which access the fracture function linked to the helicity distribution.

Back Up

Twist-3 PDF Flavor Dependence

Proton Target

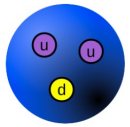

$$A_{LU,\mathbf{p}}^{\text{twist 3}} \propto 4xe^{u_V}(x) - xe^{d_V}(x)$$

Deuteron Target

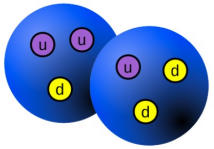

$$A_{LU,\mathbf{d}}^{\text{twist 3}} \propto xe^{u_V}(x) + xe^{d_V}(x)$$

Ongoing full partial wave analysis and comparison between proton and deuteron targets could lead to the flavor decomposition of the scalar PDF.

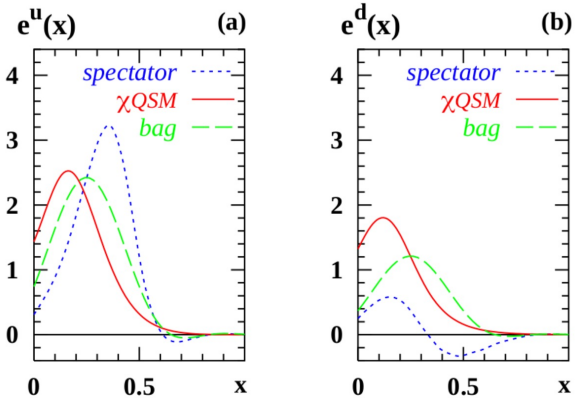

Bag Model: Nucl.Phys.B 375 (1992) 527-560
Nucl.Phys.B 497 (1997) 415-434
Spectator Model: Nucl.Phys.A 626 (1997) 937-965
Chiral Quark Soliton Model (χQSM): Acta Phys.Polon.B 39 (2008) 609-640

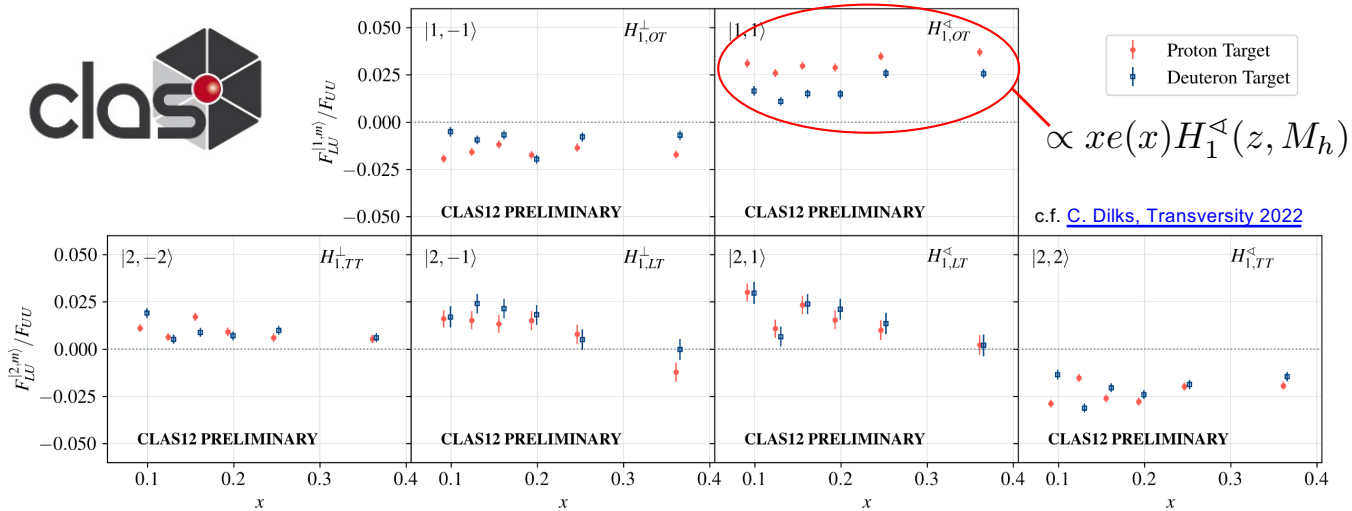

$$\propto xe(x)H_1^{\sphericalangle}(z, M_h)$$

c.f. C. Dilks, Transversity 2022

Run Period Properties

- RGA Fall 2018, inbending:
  `/cache/clas12/rg-a/production/recon/fall2018/torus-1/pass1/v1/dst/train/nSidis`
- RGA Fall 2018, outbending:
  `/cache/clas12/rg-a/production/recon/fall2018/torus+1/pass1/v1/dst/train/nSidis`
- RGA Spring 2019, inbending:
  `/cache/clas12/rg-a/production/recon/spring2019/torus-1/pass1/v1/dst/train/nSidis`
- RGB Spring 2019, inbending:
  `/cache/clas12/rg-b/production/recon/spring2019/torus-1/pass1/v0/dst/train/sidisdvcs`
- RGB Fall 2019, outbending:
  `/cache/clas12/rg-b/production/recon/fall2019/torus+1/pass1/v1/dst/train/sidisdvcs`
- RGB Spring 2020, inbending:
  `/cache/clas12/rg-b/production/recon/spring2020/torus-1/pass1/v1/dst/train/sidisdvcs`

Period	Run Range	Torus Polarity
RGA Fall 2018	5032–5419	Inbending
	5422–5666	Outbending
RGA Spring 2019	6616–6783	Inbending
RGB Spring 2019	6156–6603	Inbending
RGB Fall 2019	11093–11283	Outbending
	11284–11300	Inbending
RGB Spring 2020	11323–11571	Inbending

TABLE III: Torus polarity for each run period.

Period	Run Range	HelicityFlip
RGA Fall 2018	5032–5666	true
RGA Spring 2019	6616–6783	true
RGB Spring 2019	6120–6604	true
RGB Fall 2019	11093–11283	false
	11284–11300	true
RGB Spring 2020	11323–11571	false

TABLE V: `HelicityFlip` setting for each run period. See Table IV for the definiti `HelicityFlip`.

Period	Run Range	Energy (GeV)
RGA Fall 2018	5032–5666	10.6041
RGA Spring 2019	6616–6783	10.1998
RGB Spring 2019	6120–6399	10.5986
	6409–6604	10.1998
RGB Fall 2019	11093–11283	10.4096
	11284–11300	4.17179
RGB Spring 2020	11323–11571	10.3894

TABLE II: Beam energies for each run period.

Period	Run Range	Polarization
RGA Fall 2018	5032–5332	0.8592 ± 0.01290
	5333–5666	0.8922 ± 0.02509
RGA Spring 2019	6616–6783	0.8453 ± 0.01474
RGB Spring 2019	6142–6149	0.81132 ± 0.01505
	6150–6188	0.82137 ± 0.01491
	6189–6260	0.83598 ± 0.01475
	6261–6339	0.80770 ± 0.01449
	6340–6342	0.85536 ± 0.01484
	6344–6399	0.87038 ± 0.01474
	6420–6476	0.88214 ± 0.01502
	6479–6532	0.86580 ± 0.01460
	6533–6603	0.87887 ± 0.01454
RGB Fall 2019	11013–11309	0.84983 ± 0.02929
RGB Spring 2020	11323–11334	0.87135 ± 0.01464
	11335–11387	0.85048 ± 0.01530
	11389–11571	0.84262 ± 0.01494

TABLE VI: Polarization and uncertainty for each run period.

Not shown today

- Today want to focus on “new” things for the flavor decomposition analysis.
- Not discussed:
  1. **Combining different beam energies** (asymmetries compatible, mean kinematics virtually identical)
  2. **Fiducial cuts** (RGA fiducial cuts used for all run periods; individually checked for applicability)
  3. **Fragmentation region cuts** (motivated by sign change seen in x_F or rapidity dependencies)
  4. **Monte Carlo** (clasdis RGA configuration used, appropriate weighting for inbending/outbending ratio required, good agreement observed)
  5. **Linear dependence of asymmetry amplitudes**; $\sin(2\Delta\phi)$ amplitude extracted simultaneously
  6. **Maximum likelihood method**; unbinned fitting technique
  7. **Contributions of unpolarized modulations**; after integration over ϕ_1 and holding ϕ_1-ϕ_2 fixed only the constant modulation remains, other modulations may “sneak in” due to nonorthogality within CLAS12 acceptance.
  8. **Repeated systematics;** particle misidentification, beam polarization, beam-charge asymmetry, charge-symmetric back ground, bin migration, estimation of radiative effects, etc. all treated the same way as previous analysis.

Electron PID, HTCC

Note: RGA “nSIDIS” uses a p_e > 2.0 GeV cut and RGB “sidisdvcs” uses a p_e > 1.0 GeV.
These plots start out by enforcing p_e > 2.0 GeV to make them directly comparable. Ultimately, we require y < 0.75.

nphe > 2

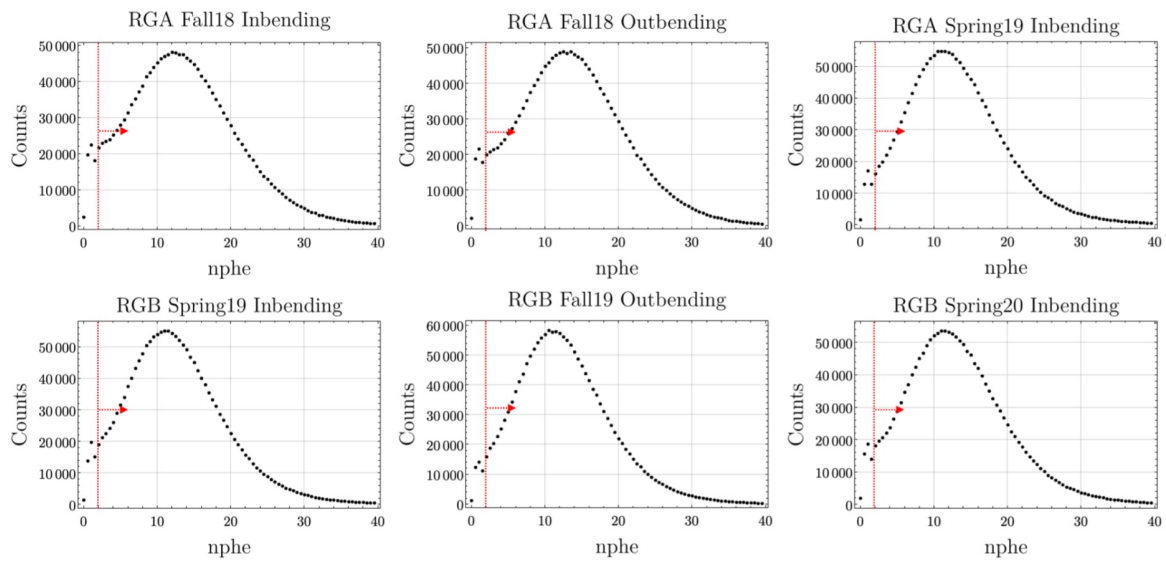

FIG. 2: Number of photoelectrons for all negative tracks in the REC::Particle HIPO bank for each run period. Vertical red lines illustrate the cut requiring more than 2 nphe for electron ID. Particles with two or fewer photoelectrons are rejected as electron candidates. A minimum momentum requirement of 2 GeV has been enforced to align the RGA and RGB trains. The distributions are largely similar, as expected.

Electron PID, PCAL Energy

Note: RGA “nSIDIS” uses a p_e > 2.0 GeV cut and RGB “sidisdvcs” uses a p_e > 1.0 GeV.
These plots start out by enforcing p_e > 2.0 GeV to make them directly comparable. Ultimately, we require y < 0.75.

nphe > 2
E_{PCAL} > 0.07 GeV

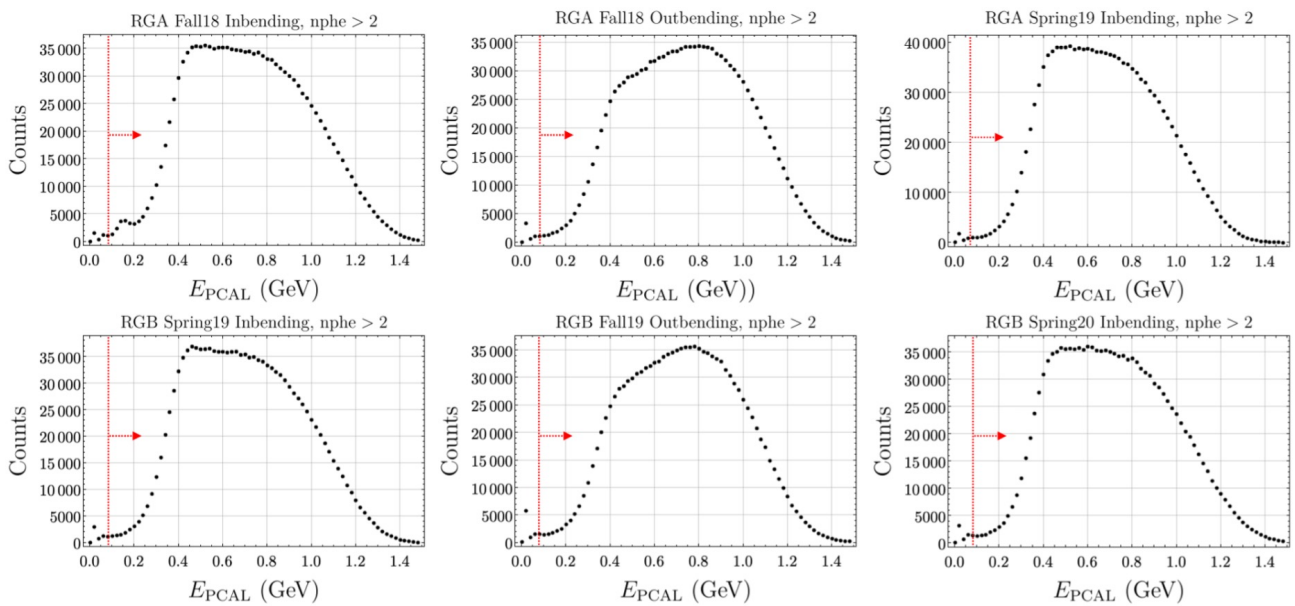

FIG. 3: Energy deposited in the PCAL by negative tracks with more than two photoelectrons detected in the Cherenkov counter. A minimum momentum requirement of 2 GeV has been enforced to align the RGA and RGB trains.

Electron PID, PCAL

Note: RGA “nSIDIS” uses a p_e > 2.0 GeV cut and RGB “sidisdvcs” uses a p_e > 1.0 GeV.
These plots start out by enforcing p_e > 2.0 GeV to make them directly comparable. Ultimately, we require y < 0.75.

Without cuts

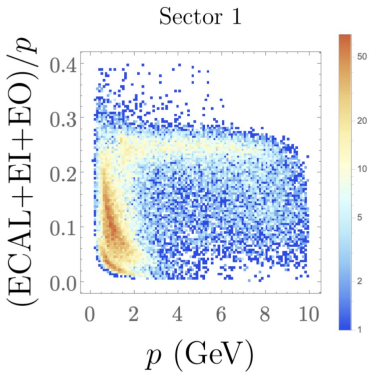

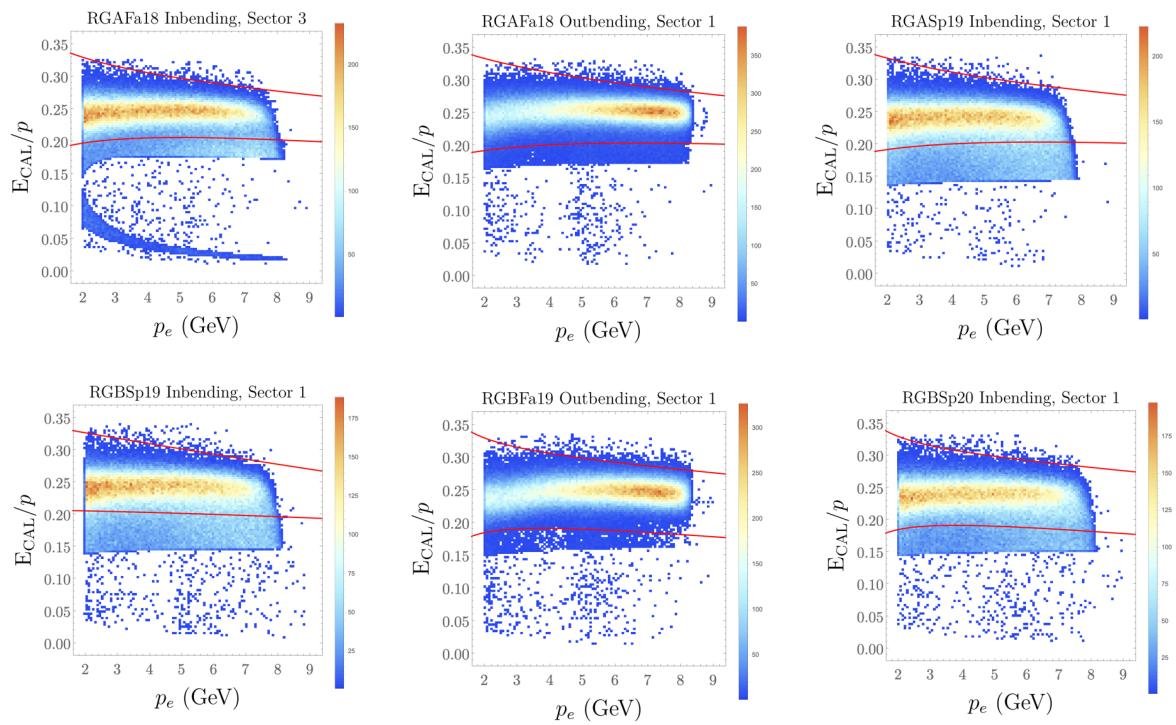

Electron PID, PCAL

Note: RGA “nSIDIS” uses a p_e > 2.0 GeV cut and RGB “sidisdvcs” uses a p_e > 1.0 GeV.
These plots start out by enforcing p_e > 2.0 GeV to make them directly comparable. Ultimately, we require y < 0.75.

Without cuts

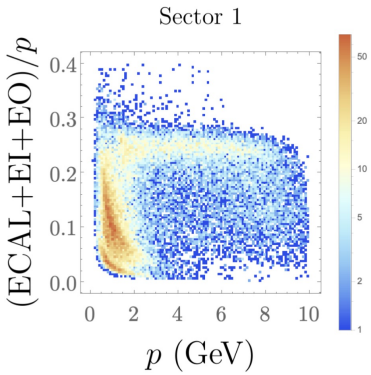

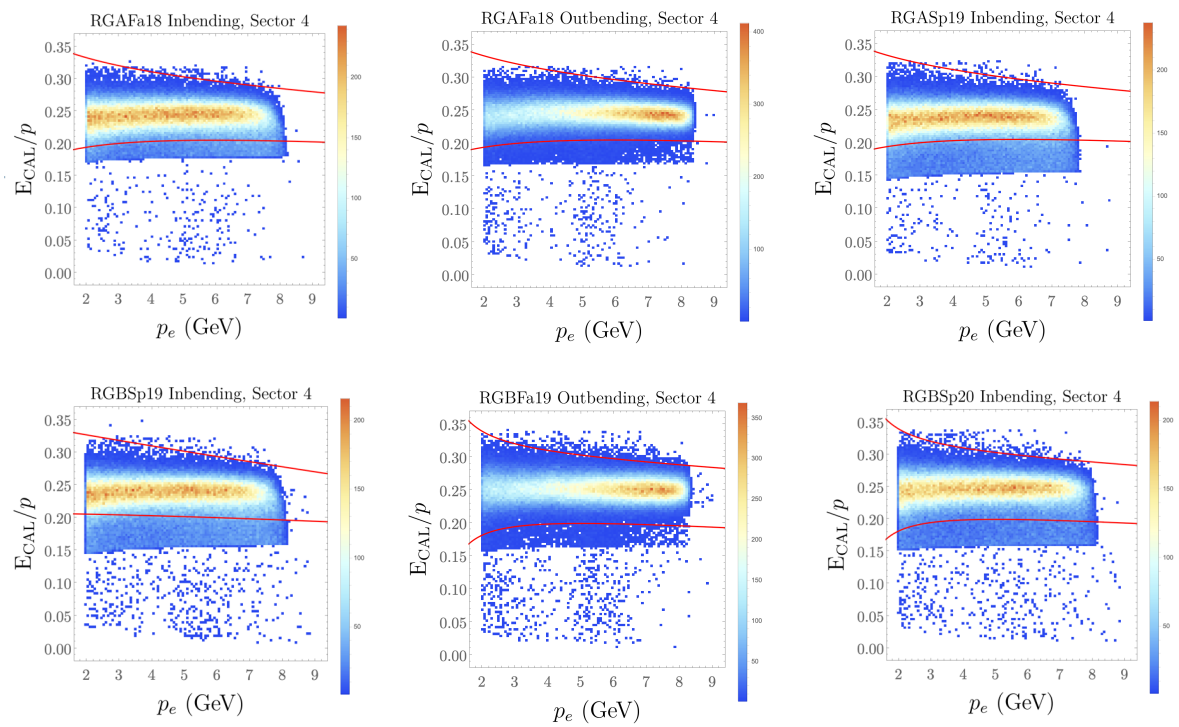

Vertex Cuts

- Target foil at ~5.5 cm added for RGBSp19 and after.
- Slightly different behavior for inbending and outbending. Equivalent behavior for RGA/RGB (same FD alignment).
- Positive(negative) tracks for inbending: $-10 < v_z < 2.5$, $(-8 < v_z < 3)$
- Positive(negative) tracks for outbending: $-8 < v_z < 3$, $(-10 < v_z < 2.5)$

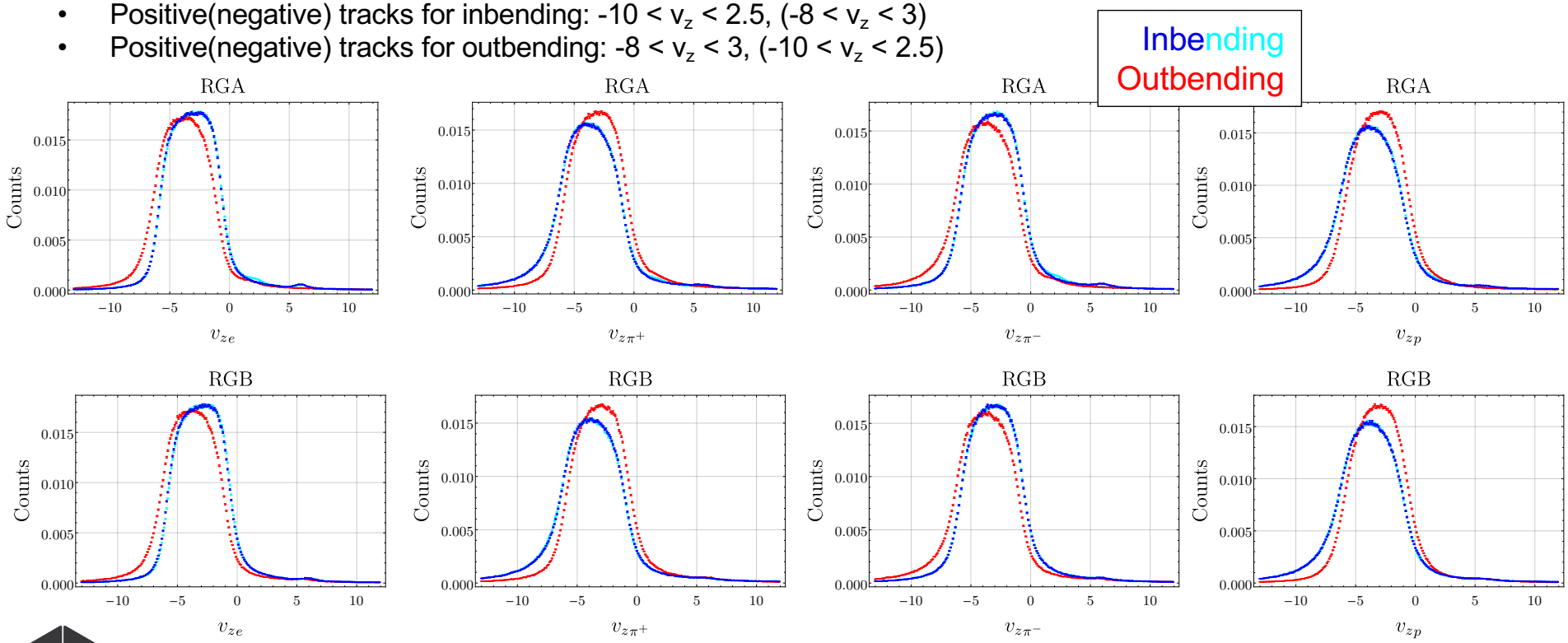

Missing Mass

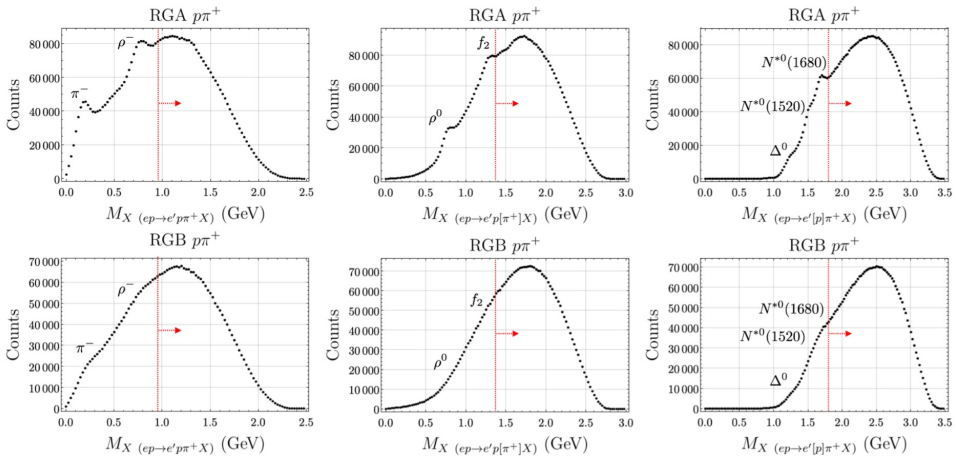

FIG. 9: Distributions of the missing mass of $ep \to e'p\pi^+X$ (first column), $ep \to e'p[\pi^+]X$ (second column) and $ep \to e'[p]\pi^+X$ (third column) for the RGA (first row) and RGB (second row) data sets. Both torus configurations have been combined.

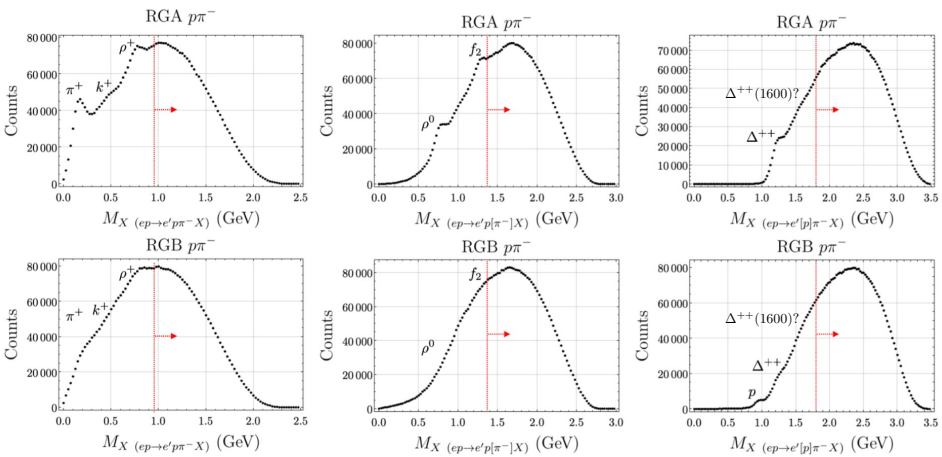

FIG. 10: Distributions of the missing mass of $ep \to e'p\pi^-X$ (first column), $ep \to e'p[\pi^-]X$ (second column) and $ep \to e'[p]\pi^-X$ (third column) for the RGA (first row) and RGB (second row) data sets. Both torus configurations have been combined.

$M_x(ep \rightarrow e'p\pi X)$

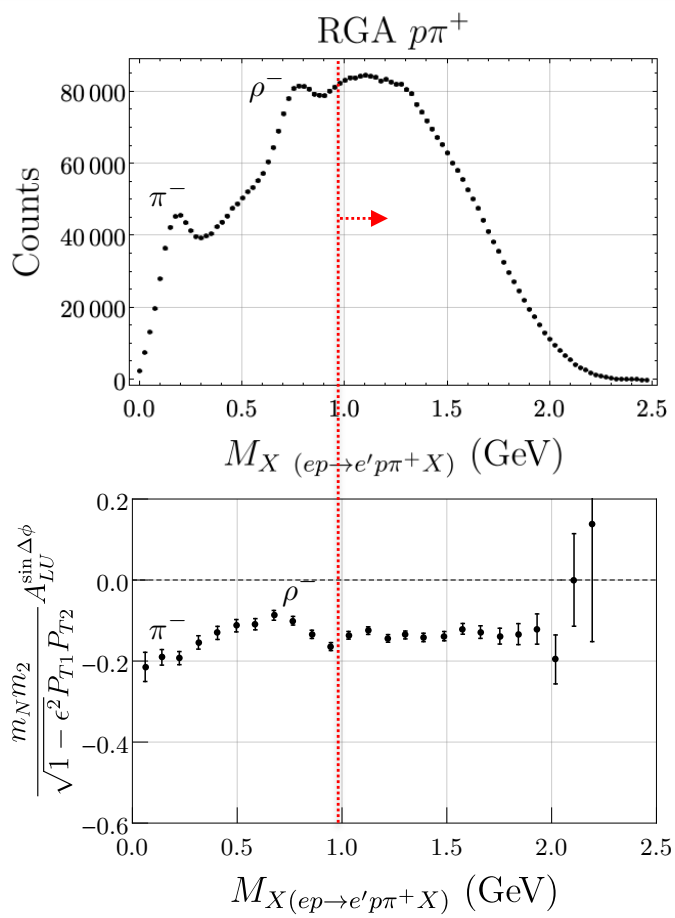

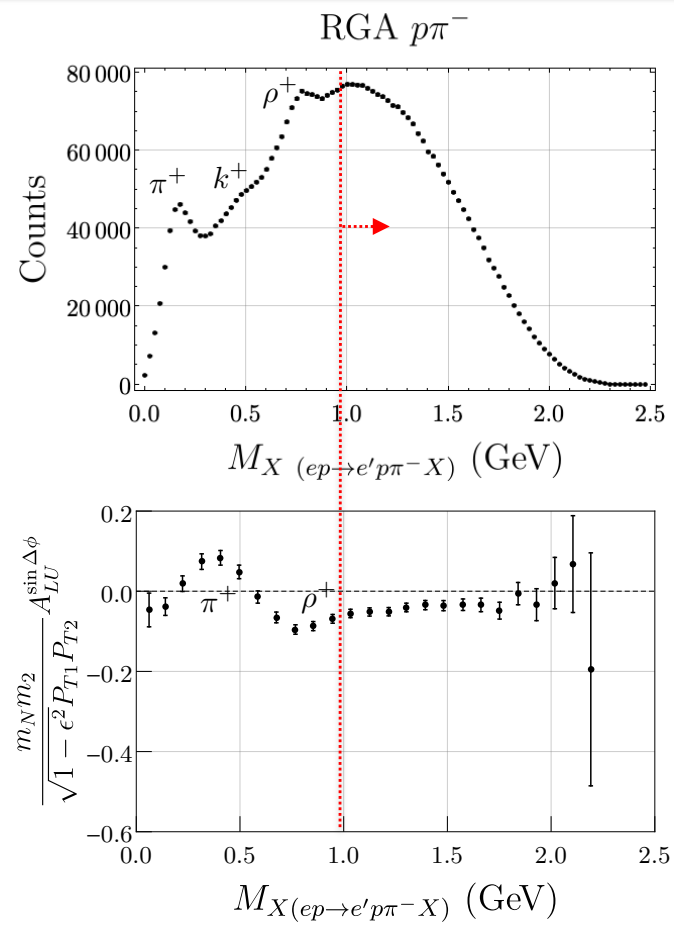

Proton Energy Loss Corrections

Proton energy loss corrections developed by UConn group.

Separate distributions above and below 27°

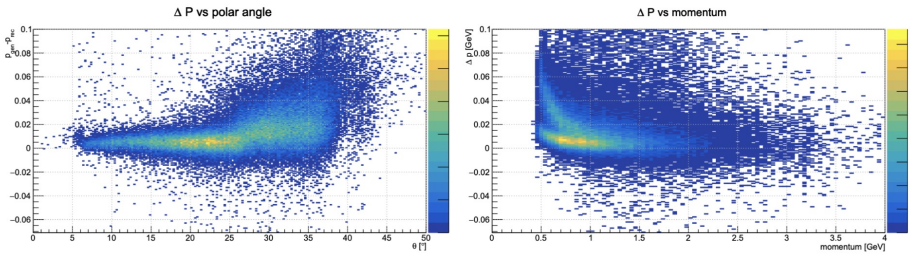

(a) ΔP as a function of θ (b) ΔP as a function of P

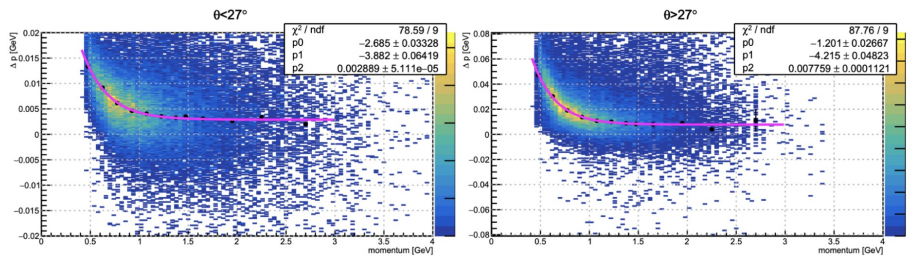

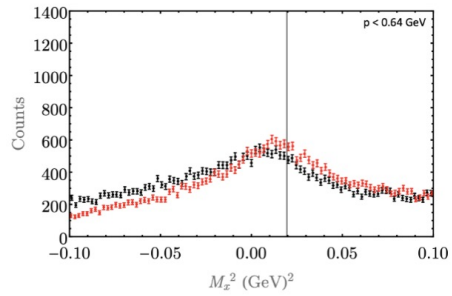

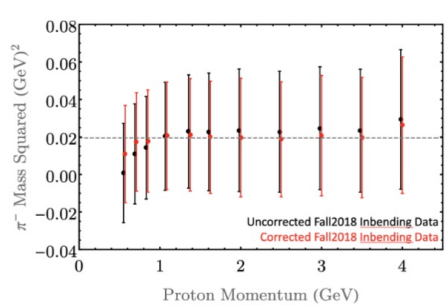

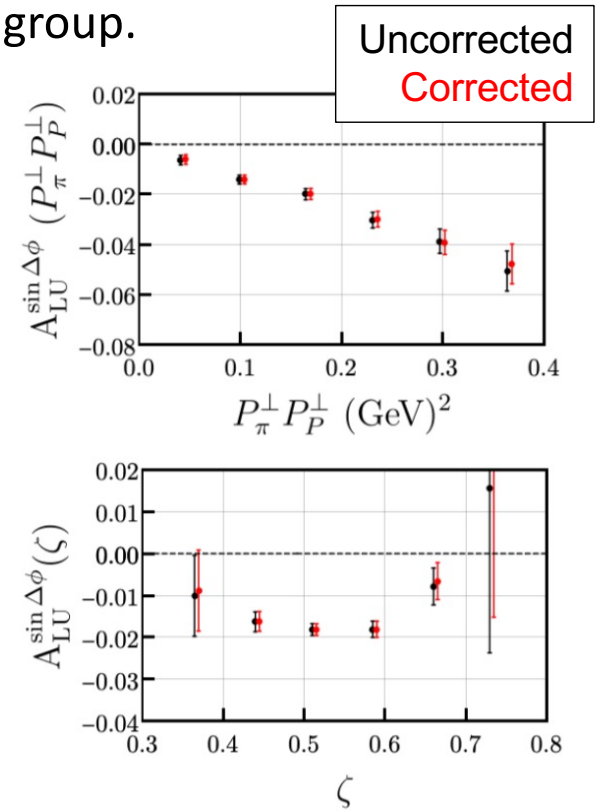

As expected for a SIDIS BSA analysis… almost no effect.

Extracting A_{LU}

- Select $ep \rightarrow e'P\,\pi^+ + X$.
- Consider all possible hadron pairs.
- Amplitudes are extracted simultaneously via maximizing a likelihood function.
- Unbinned maximum likelihood method:

$$-\ln \mathcal{L}_{ML}(A) = N - \sum_i^N \ln\left[1 + h_i P_i \left(A_1 \sin\Delta\phi_i + A_2 \sin 2\Delta\phi_i\right)\right]$$

- Extension in place to sum over MC in order to estimate UU contributions… needs work
- Include relevant beam polarization and kinematic factors on an event-by-event basis in the likelihood fit.

Channel selection
- Q^2>1.0 GeV^2
- W>2.0 GeV
- M_x>0.95 GeV
- M_{x1}>1.35 GeV
- M_{x2}>1.80 GeV
- y<0.75
- $\Delta Y > 0$
- $x_{f1} > 0$
- $x_{f2} < 0$
- $z_1 > 0.2$

Balancing Yields

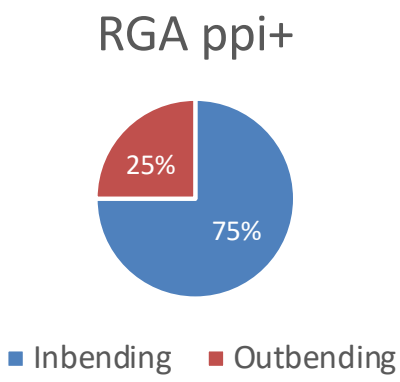

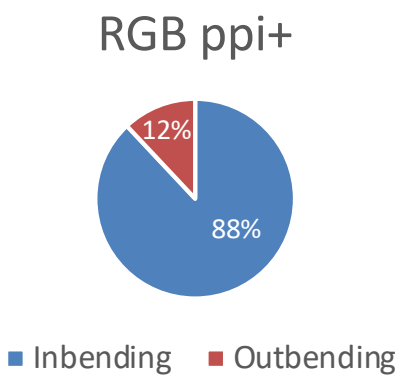

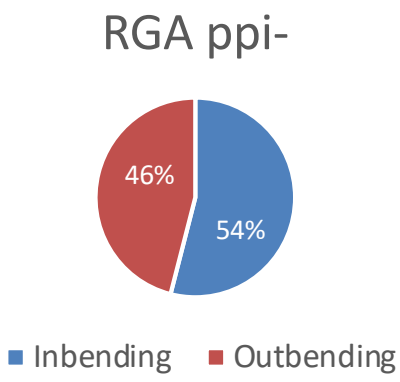

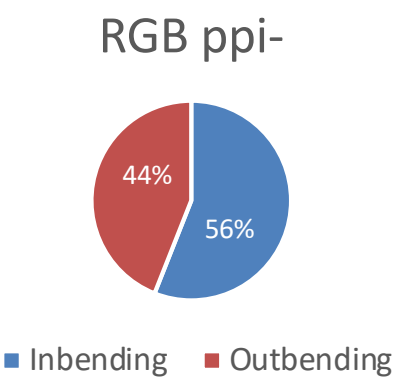

- Yields are relatively similar and as will be seen the distributions match up nicely, not worth doing a complicated weighting system.
- Still, four separate measurements and each measurement will report mean Q^2, x, z, etc. etc.

Comparison between RGA and RGB

- Very minor differences in distributions sensitive to energy (<RGA> > <RGB>) and torus (RGA In < RGB In).
- Variables not directly sensitive to these differences (e.g. z_1, x_F) are identical.

RGA $p\pi^+$
RGB $p\pi^+$

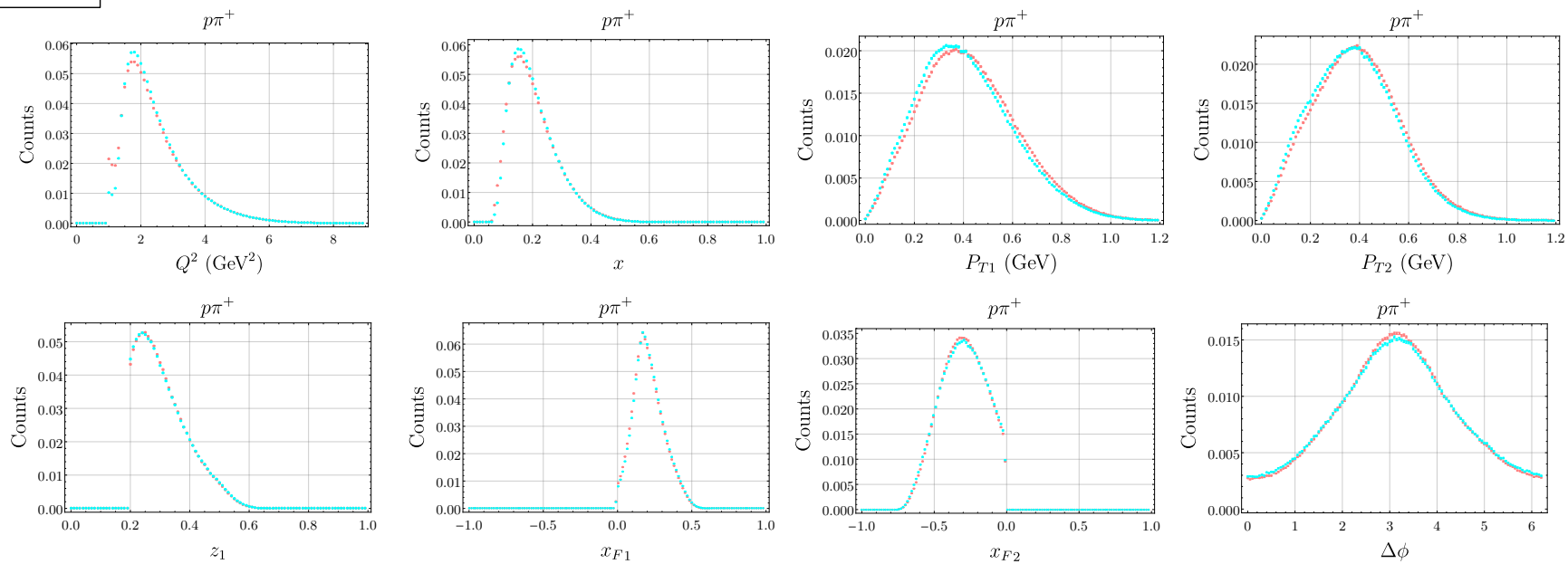

Comparison between RGA and RGB

- Very minor differences in distributions sensitive to energy (<RGA> > <RGB>) and torus (RGA In < RGB In).
- Variables not directly sensitive to these differences (e.g. z_1, x_F) are identical.

RGA $p\pi^-$
RGB $p\pi^-$

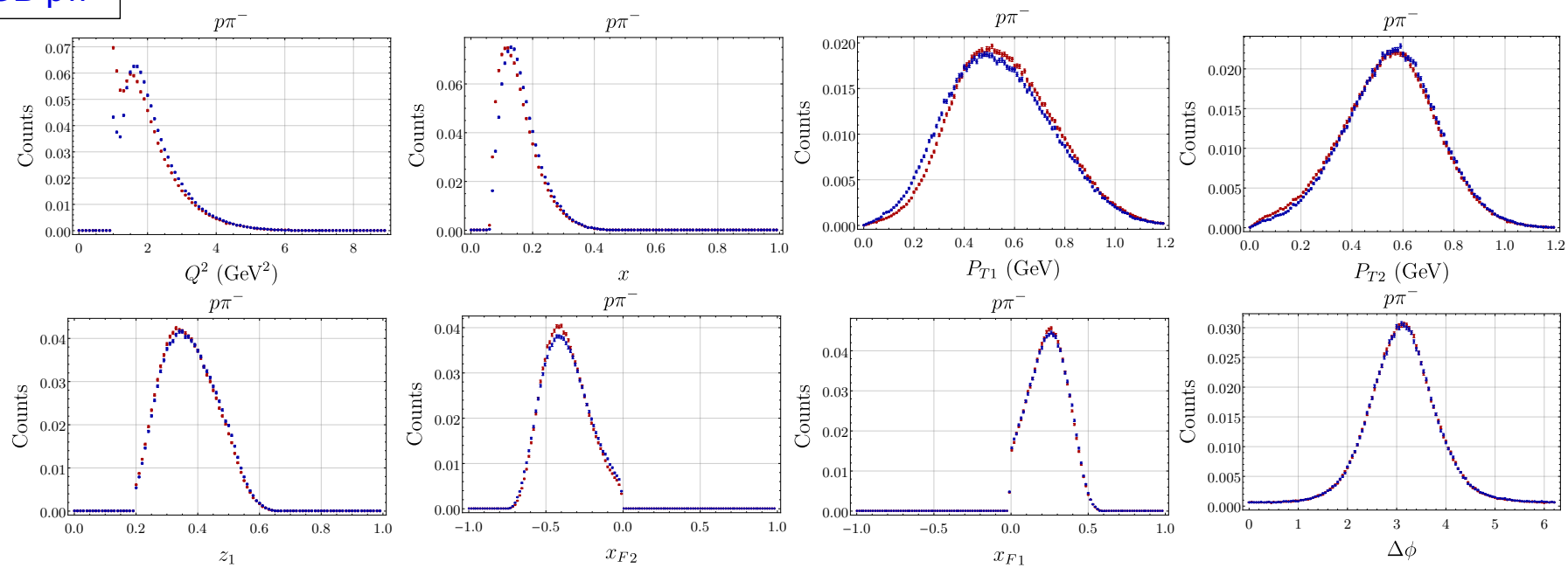

Data vs MC (ppi+)

- Significantly more inbending MC than outbending MC – just throw away inbending MC until the ratios match the data.
- clasdis only mass produced for proton target but as RGA ≈ RGB and RGA Data ≈ RGA MC this should be fine.

RGA Data
RGA MC

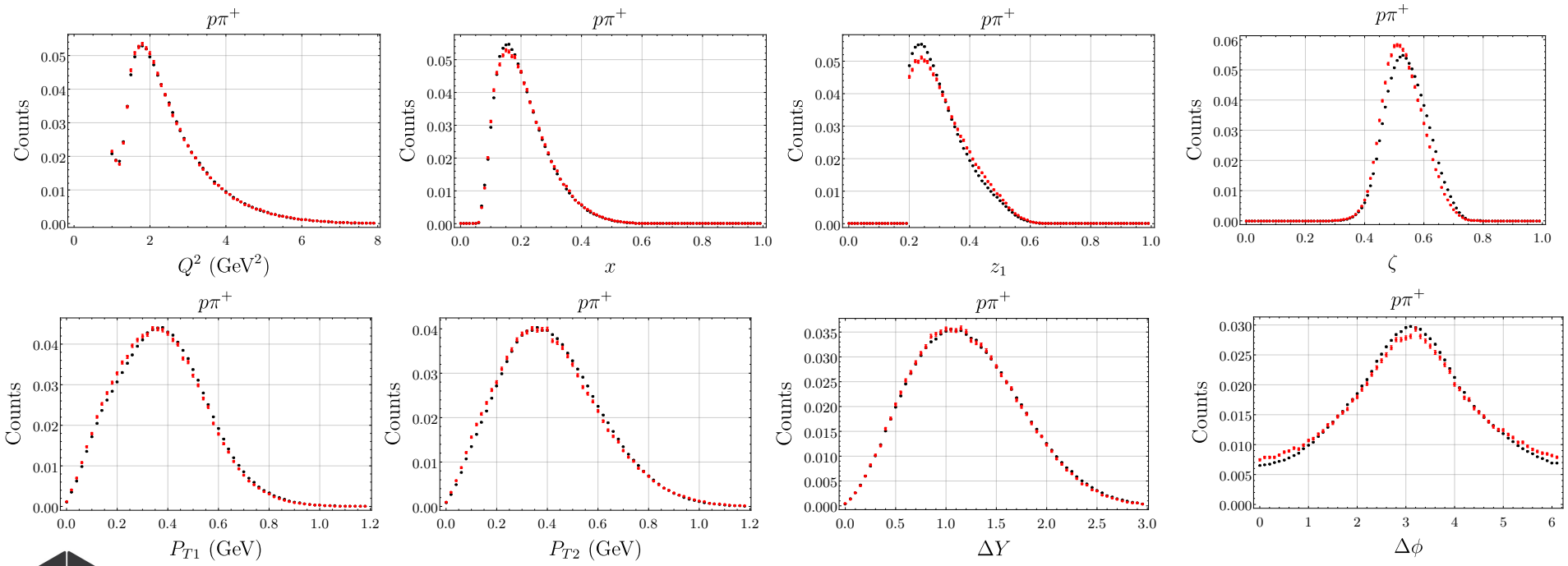

Data vs MC (ppi-)

- Significantly more inbending MC than outbending MC – just throw away inbending MC until the ratios match the data.
- clasdis only mass produced for proton target but as RGA ≈ RGB and RGA Data ≈ RGA MC this should be fine.

RGA Data
RGA MC